

# The Dendrimer Effect in Homogeneous Catalysis

Brett Helms<sup>a</sup> and Jean M. J. Fréchet<sup>a, b, \*</sup>

<sup>a</sup> Department of Chemistry, University of California, Berkeley, CA 94720, USA

Fax: (+1)-510-643-3079; e-mail: frechet@berkeley.edu

<sup>b</sup> Material Sciences Division, Lawrence Berkeley National Laboratory, Berkeley, CA 94720, USA

Received: March 12, 2006; Accepted: May 10, 2006

**Abstract:** The immobilization of catalytic groups onto a dendritic support either at the core or at the periphery gives rise to unique properties that affect rates of reaction, substrate activation or selectivity, etc. When advantageous, these properties can be classified as a positive dendrimer effect. Positive dendrimer effects can arise from site isolation, transition state stabilization and/or dielectric effects in the case of core-modified dendrimers, while peripherally modified dendrimers usually benefit from steric crowding or cooperativity for catalytic residues confined to the surface of the polymer. In this review, the appearance of positive dendrimer effects from

the literature will be highlighted as well as prospects for future work in the field.

- 1 Introduction
- 2 Commonly Used Dendrimer Platforms for Macromolecular Catalysts
- 3 Core-Functionalized Dendrimers in Catalysis
- 4 Peripherally Modified Dendrimers in Catalysis
- 5 Conclusion and Outlook

**Keywords:** cooperative effects; dendrimers; homogeneous catalysis; structure-activity relationships; supported catalysts

## 1 Introduction

In the interest of “green chemistry”<sup>[1]</sup> and atom economy,<sup>[2]</sup> molecular catalysis remains an active area of research in both academia and industry, primarily for the production of fine chemicals used in agriculture, drug manufacture, organic electronics, etc. Solution-based methodologies rely not only on the discovery and optimization of small molecule catalysts for a given transformation, but also on efficient means to separate the desired product(s) from the catalyst and any by-products in the reaction mixture. While this process can be facilitated by using heterogeneous catalysts, i.e., catalysts immobilized onto organic or inorganic solid supports such as silica or cross-linked polymeric beads, there are several drawbacks to this approach that generally limit its widespread application to batch processes. These drawbacks include non-uniformity in catalyst structure and microenvironment once it is immobilized onto the support material, slow diffusion of substrates therein, catalyst leaching, and lower overall activities than the homogeneous system.<sup>[3]</sup> Solid polymeric supports also exhibit limited swelling ability in certain solvents. Efforts to overcome these disadvantages have primarily been directed at using soluble polymers for catalyst immobilization.<sup>[4]</sup> In this manner, the desirable features of homogeneous catalysis, such as comparable reaction kinet-

ics and mass transfer, can be maintained while the macromolecular nature of the material provides a convenient means of purification and, in some cases, recyclability (*vide infra*).

Both linear polymers and various families of branched polymers have been used as soluble macromolecular supports for reagents and catalysts. While the former are, in general, more readily available, they can suffer from poor loading capacity. It is common for only one catalyst moiety to be appended to the end of a linear polymer, such as monomethoxy-poly(ethylene glycol) (MeO-PEG). For example, MeO-PEG<sub>5000</sub> catalyst conjugates carry a loading of only 0.2 mmol catalyst per gram of polymer while branched polymers typically carry several mmol g<sup>-1</sup> when the degree of branching is greater than 50%.<sup>[5]</sup> In the case of dendrimers, where the degree of branching is 100%, the highest possible loading can be achieved. Certainly, in the literature, there has been extensive work to optimize the catalytic activity of functional dendrimers to mimic that of the small molecule, but with the inherent retention ability that accompanies immobilization on macromolecular supports. There are both covalent<sup>[6]</sup> and non-covalent<sup>[7,8]</sup> approaches described in the literature and many of these have been used in continuous flow membrane reactors (CFMRs) with high efficacy.<sup>[7,9]</sup> The dendrimer catalysts in these studies exhibited a rather high

*Brett Helms* was born in California (USA) in 1978. He earned a BS in Chemistry from Harvey Mudd College (Claremont, CA) in 2000. His PhD was completed in 2006 at the University of California, Berkeley under the supervision of Professor Jean M. J. Fréchet. His interests include the synthesis and application of macromolecules with well-controlled, highly branched architectures as novel materials for homogeneous catalysis. Such macromolecules have included dendrimers, dendronized linear polymers, and multi-arm star polymers. He currently holds a postdoctoral position at the Technische Universiteit Eindhoven in the group of E. W. Meijer studying multivalent protein-protein interactions using dendritic polymers.



*Jean Fréchet* received his first university degree at the Institut de Chimie et Physique Industrielles (now CPE) in Lyon, France, and PhD degrees from SUNY College of Forestry and Syracuse University. His academic career has included 14 years on the chemistry faculty of the University of Ottawa in Canada, and ten years at Cornell University. He is currently Professor of Chemistry and Chemical Engineering at the University of California, Berkeley where he holds the Henry Rapoport Chair of Organic Chemistry, and directs the Organic and Macromolecular Facility at the Molecular Foundry, Lawrence Berkeley National Laboratory. His research at the interface of organic, biological, and materials chemistry is directed towards functional polymers, their design, synthesis, and applications.



degree of active site stability and independence (i.e., neither cooperative nor non-cooperative effects were observed) for a variety of catalytic groups placed at the polymer surface, even for the larger dendrimers.

In some cases, however, high catalyst loading and reactivity comparable to the parent catalyst are not the main objectives of polymer attachment. Instead, immobilization of the catalyst onto a polymer is expected to give rise to certain properties that are not possible otherwise. Such properties might include enhanced stability through steric isolation, cooperativity through proximal confinement of reactive groups, or catalyst tuning through dielectric effects exerted by its nanoenvironment. These properties are uniquely afforded by systems employing branched polymers, particularly dendrimers, since their syntheses generally produce well-defined materials with a high degree of structural control and placement of functional groups throughout the macromolecule.<sup>[10]</sup> In this review, we will discuss the unique role of polymer topology in controlling the performance of soluble polymers in homogeneous catalysis with an emphasis on macromolecules with a dendritic architecture. The special properties that may result from catalyst incorporation onto these macromolecules can be described as a “dendrimer effect.” This term has been generally invoked in the literature to explain phenomena that arise as the generation of dendrimer increases. In the examples that follow, special attention is given to those wherein a beneficial or “positive” dendrimer effect has been observed. From these examples, several common themes begin to emerge and these have

been gathered in this rather comprehensive, if qualitative, description of the dendrimer effect in catalysis.

## 2 Commonly Used Dendrimer Platforms for Macromolecular Catalysts

The catalytic properties of branched polymer supports used in homogeneous catalysis are modulated by the specific polymer topology, i.e., linear or branched architecture. Polymer topology may determine the number and relative spatial arrangement of immobilized catalytic moieties in solution. The chemical nature of the support may also affect the rate of reaction through dielectric effects and through its interaction with the substrate(s) and product(s), thereby affecting mass transfer. These effects have been noted in the literature since the first Merrifield resins were used in solid-phase synthesis applications in the 1960s.<sup>[11]</sup> Until now, however, the effects have been hard to quantify without reliable and precise chemical means of controlling polymer microstructure and topology through organic synthesis.

Recently, chemical approaches to control polymer topology have been successful using convergent<sup>[12]</sup> and divergent<sup>[13]</sup> syntheses to prepare dendrimers, while slow-addition protocols can be used to obtain hyperbranched polymers.<sup>[14]</sup> Controlled syntheses of star polymers<sup>[15]</sup> have also been put forth, and dendronized linear polymers<sup>[16]</sup> have benefited from the methods developed for their spherical dendrimer

counterparts. Each of these architectures has advantages and disadvantages that may be related to the degree of structural perfection achieved or to the ease of preparation and characterization of the material. For example, a high polydispersity has negative implications on the characterization of catalyst activity, due to structural non-uniformity, and generally prevents the application of the macromolecular catalyst in CFMRs. The scale on which the polymer synthesis is carried out is also an important factor when considering its implementation in an industrial process.

Because of their near structural perfection, dendrimers are arguably the most well-suited of the branched polymer architectures for catalysis applications. Dendrimers display hierarchical conformational ordering at various stages of their growth, eventually reaching globular conformations at higher generations.<sup>[17]</sup> These prescribed changes in structure with increasing generation provide a convenient basis for rationalizing the catalytic behavior for a series of related dendrimer catalysts. This would be near impossible with other branched polymer architectures that are statistical ensembles of active species. Other advantages of dendrimers are related to their monodispersity, their uniformity in catalyst structure, and their precise syntheses. For example, their iterative synthesis allows for the placement of catalytic groups at any point resulting in a functional macromolecule with a rather well characterized structure.<sup>[18]</sup> A survey of dendrimer types commonly used in catalysis applications is shown in Figure 1. Typically, catalyst residues have been appended to the structures either at the core, at each branch point, or at the periphery. Positive dendrimer effects arising from each of these catalyst arrangements have been documented in the literature and will herein be discussed.

Apart from architecture, the chemical make-up of the dendritic polymer can affect various aspects of catalysis (*vide infra*). There are several dendritic platforms that have found widespread use in catalysis applications (Figure 2): polyamidoamines<sup>[19]</sup> (PAMAM), polypropylene imines<sup>[20]</sup> (PPI), polybenzyl ethers<sup>[21]</sup> (Fréchet-type), polyaliphatic esters,<sup>[22]</sup> polycarbo-

silanes<sup>[23]</sup> and polyester amides<sup>[24]</sup> (Newkome-type). The selection of one platform over another may be made for reasons of synthetic convenience, to accommodate the reaction conditions, or to achieve a specific nanoenvironment that could influence the overall catalytic process.

### 3 Core-Functionalized Dendrimers in Catalysis

The steric crowding of reactive core moieties upon dendritic encapsulation remains one of the more challenging obstacles to overcome in catalysis. In general, slower rates of reaction with increasing dendrimer generation are observed when core-confined catalysts are so isolated from the reaction medium. A quantitative treatment of this phenomenon was recently reported by the groups of Cossio and Lopez.<sup>[25]</sup> In their work, a single tertiary amine catalyst for the Henry (nitroaldol) reaction was encapsulated by a series of dendrimers of different generation (G0 to G2) with different branch multiplicities. Dendrimer catalysts **1**, **2** and **3** derived from A-B<sub>3</sub> monomer types are shown in Scheme 1. Pseudo-first-order rate constants,  $k_{obs}$ , for the reaction between benzaldehyde and 2-nitroethanol were measured for these families of dendrimers *via in situ* FT-IR measurements. It was shown that the catalytic ability of a single active site in this reaction decreased both with higher generation and with higher branching multiplicity. For example, the  $k_{obs}$  values for dendrimers **1**, **2** and **3** were 12.11, 1.89 and  $1.03 \times 10^{-4} \text{ s}^{-1}$ , respectively. The authors further characterized the structure-activity profiles for these dendrimers using molecular dynamics simulations. A linear relationship was observed between the relative collision rates of the dendrimers and an expression involving the dendrimer's "reagent accessible surface" and its molecular weight. In addition, the slope of that line was used to determine any (non-)cooperative effects brought about by encapsulation through a comparison to the slope of the line drawn to represent ideal behavior in which the polymer does not participate in any way in the reaction. The negative linear departure from ideal behavior observed in this system clearly indicated the deleterious kinetic effects that accompany dendritic encapsulation when there is no direct participation by the polymer backbone to the catalytic cycle, substrate binding, or mass transfer. These results may offer insight to so-called "negative dendrimer effects" found in the literature.<sup>[26]</sup>

While steric shielding of reactive groups at the core of dendrimers usually carries negative kinetic consequences, there are several instances in which the globular polymer shell proves advantageous. The incorporation of monodentate ligands such as pyri-

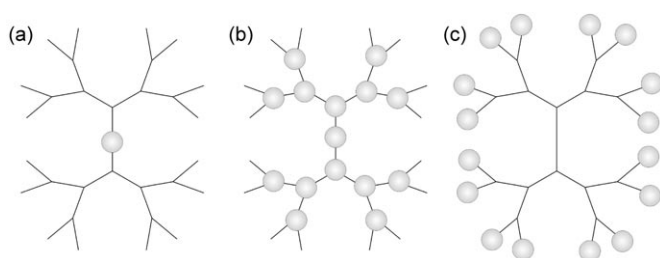


**Figure 1.** Commonly encountered catalyst placement on dendritic polymer supports: (a) core-functionalized dendrimers; (b) dendrimers with modified branch points; and (c) peripherally modified dendrimers.

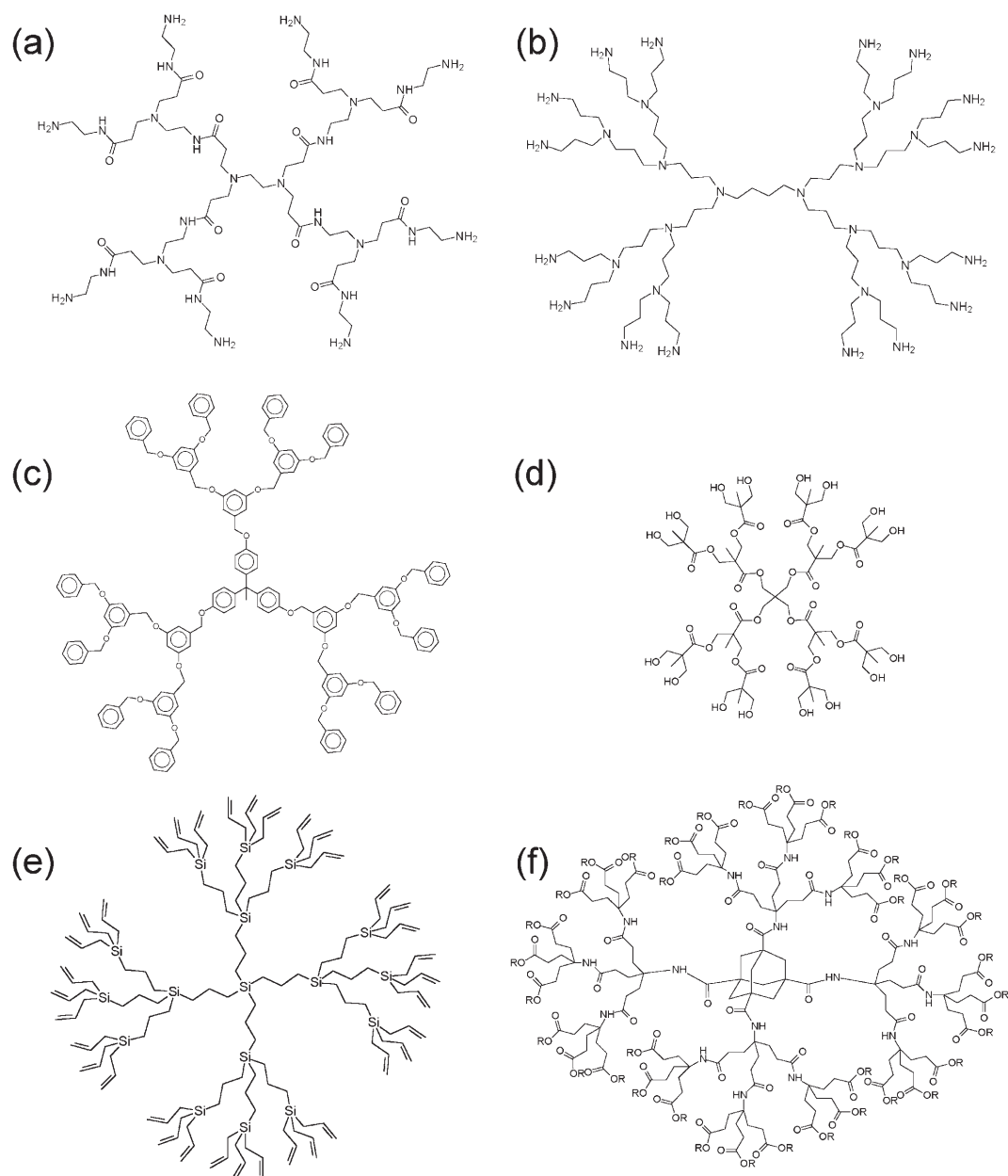
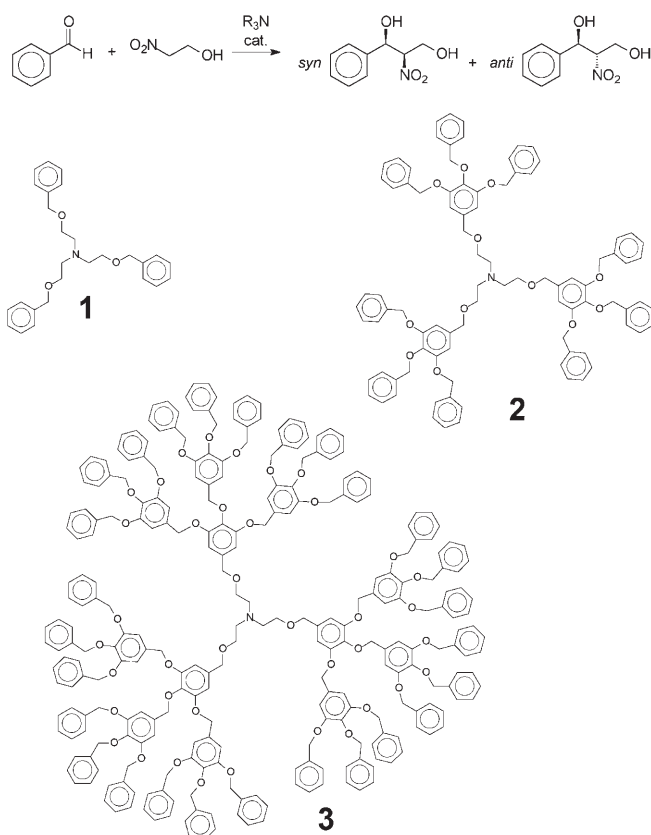


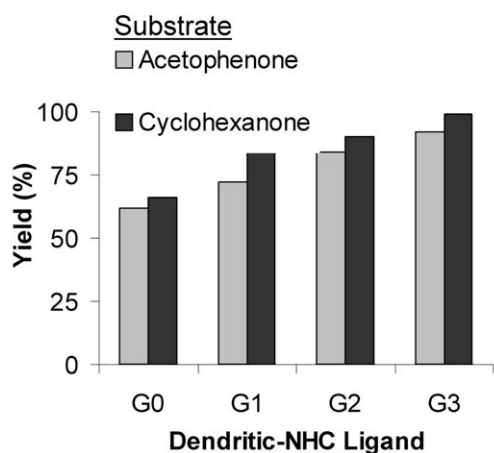
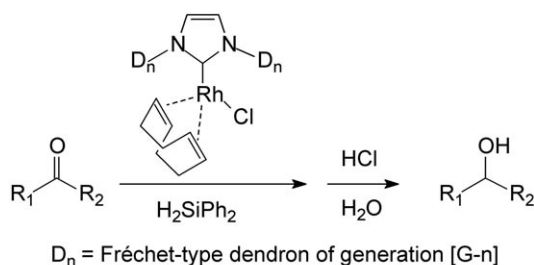
**Figure 2.** Structures of dendrimers commonly used in catalysis: (a) PAMAM; (b) PPI; (c) polybenzyl ether; (d) polyaliphatic ester; (e) polycarbosilane; and (f) polyester amide.

dines and phosphines into the interior of dendrimers has, in general, been found to enhance the stability of transition metal complexes derived thereof in the presence of air and/or other agents that might otherwise lead to catalyst deactivation.<sup>[27,28]</sup> In some cases, catalysts at the cores of these dendrimers suffer a concomitant loss of activity due to steric crowding of the active site. However, in cases where stability is the dominant factor in determining activity, dendronization becomes an extremely attractive approach to derive maximum activity from the expensive metals.

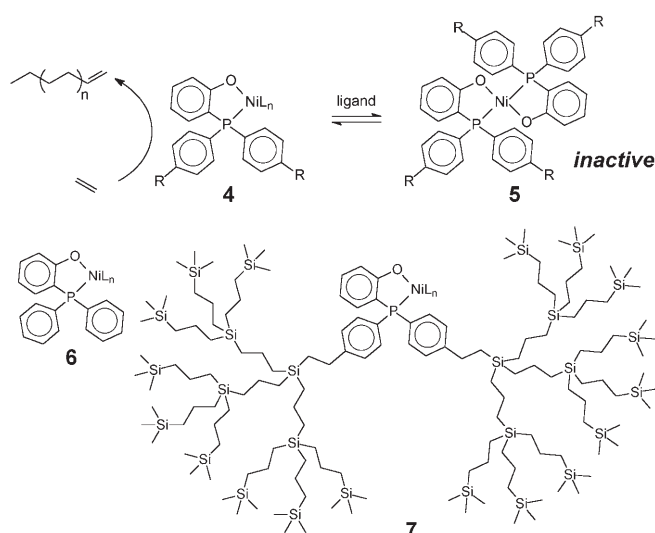
Due to their strong bond with metals, N-heterocyclic carbene (NHC) ligands are very desirable and have been shown to be extremely versatile in their applicability to a variety of organic transformations.<sup>[29]</sup> Rhodium(I) complexes bearing NHC ligands derived from their imidazolium salts have been used in hydrosilylation reactions of ketones under mild conditions, although these reactions are usually limited by factors such as catalyst stability and activity. Tsuji et al. have reported the use of dendritic NHC ligands in the Rh(I)-catalyzed hydrosilylation of acetophenone and cyclohexanone (Scheme 2).<sup>[30]</sup> A positive dendrimer



**Scheme 1.** Henry reaction between benzaldehyde and 2-nitroethanol using single site dendritic tertiary amine catalysts.



**Scheme 2.** Hydrosilylation of ketones by dendritic NHC-Rh(I) catalysts.



**Scheme 3.** Ethylene oligomerization using P,O-Ni complexes. Formation of a bis(P,O)-Ni adduct results in catalyst deactivation.

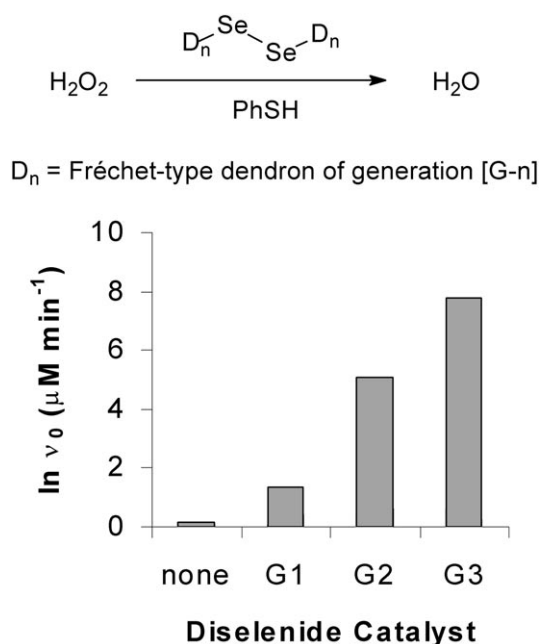
effect resulting in an increase in the yield with increasing generation of the  $\text{Rh}^{\text{I}}$  complex was observed. This effect was attributed to the folding of the dendrimer around the active site that led to greater stability and hence greater overall turnover during the course of the reaction.

While the previous example invoked a single dendritic ligand in the catalyst system, it is also common for multiple ligands to be present at a catalytically active metal center. In those instances, various equilibria are involved when the catalyst is formed *in situ* from metal precursors and excess ligand. Indeed, several catalytic species may be present in solution, and because of their different ligand environments, they may possess different activities. It is also conceivable that core-functionalized dendrimer ligands could alter these equilibria due to excluded volume effects brought about by the assembly of multiple ligands to the metal center; because of their smaller size, such a phenomenon would not be experienced with the parent ligand. For example, nickel complexes bearing P,O ligands, such as *o*-phenylphosphinophenols, have been used widely in industry, for example, in the Shell higher olefin process.<sup>[31]</sup> Reactions involving these nickel complexes are usually carried out in non-polar solvents such as toluene, although the use of more environmentally benign media has also been explored; however, in polar solvents like alcohols or water, there is a strong tendency for the formation of a bis-(P,O)nickel complex **5**, which is inactive (Scheme 3). In their work, van Leeuwen and co-workers have constructed a second generation dendritic P,O ligand **7** based on a carbosilane platform that was effective in preventing undesirable bis(P,O)nickel complexes in toluene.<sup>[32]</sup> As a consequence of this site isolation, the



dendritic ligand **7** ( $\text{TOF}_{\text{avg}} = 7700 \text{ h}^{-1}$ ) outperforms the parent ligand **6** ( $\text{TOF}_{\text{avg}} = 3600 \text{ h}^{-1}$ ) in ethylene oligomerization leading to higher yields of oligoethylene. The site isolation provided by the dendritic ligand **7** is mitigated in methanol as bis(P,O)nickel complexes are observed. However, the second P,O ligand appears to be labile at higher reaction temperatures, which is not the case with ligand **6** and its bis-(P,O)nickel complex. As a result, the nickel catalyst based on the dendritic ligand shows good activity ( $\text{TOF}_{\text{avg}} = 3242 \text{ h}^{-1}$ ) in methanol whereas the parent ligand itself (**6**) does not produce any higher olefins.

Apart from providing site isolation, the globular dendritic architecture around a catalytically active site also functions to bind guest molecules, another important factor for achieving efficient catalysis. Many early reports of small molecule binding by dendrimers focused on dye molecules as reporter probes,<sup>[33]</sup> although substrate molecules can be treated similarly when catalysis applications are considered. This aspect of catalysis with dendrimers is reminiscent of molecular transformations achieved by enzymes in which substrate binding features prominently in determining the substrate selectivity and the extent of product inhibition.<sup>[34]</sup> The simple model describing the active site of an enzyme as a hydrophobic binding pocket for substrates held in close proximity to moieties that perform the transformation has often been applied, with mixed success, to hydrophobic, sometimes amphiphilic, dendrimers. As described earlier, steric congestion resulting from the encapsulation of reactive groups within the dendrimer frequently leads to slower kinetics,<sup>[25]</sup> however, there are notable exceptions: for instance, when substrate binding ability and nanoenvironment effects are paramount to achieving reactivity. In this respect, binding pockets with the desired characteristics will be found only in the larger dendrimers. A nice example of this phenomenon was reported recently by Zhang et al. with a series of Fréchet-type poly(benzyl ether) dendrimers with a diselenide core that demonstrate generation-dependent glutathione peroxidase (GPx) activity (Scheme 4).<sup>[35]</sup> The catalytic cycle involves the reduction of hydrogen peroxide by benzenethiol in the presence of diselenide-cored dendrimers. Substrate binding was found to increase with dendrimer generation ( $K_a = 16.4$ ,  $39.4$  and  $252.7 \text{ M}^{-1}$  for G1, G2 and G3, respectively). A similar increase was noted for the initial rates of peroxide reduction ( $\nu_0 = 4.07$ ,  $8.19$  and  $2431.20 \text{ } \mu\text{M min}^{-1}$  for G1 to G3, respectively). As a point of reference, the authors showed that the third generation catalyst performed around 1400 times faster than Ebselen,<sup>[36]</sup> a small molecule antioxidant previously studied as a GPx mimic. Higher activities for the dendrimers were achieved upon the introduction of small amounts of water into the reaction medium, presumably as a result of stronger binding of



**Scheme 4.** Peroxide reduction by dendritic diselenides.

the substrate to the dendrimer due to the hydrophobic effect. This study points to the importance of nanoenvironment effects in dendrimer catalysts where substrate binding requires larger dendrimers that are able to provide the more hydrophobic environment best suited for the reaction.

Substrate binding can also be achieved through specific molecular interactions, such as ion pairing. Highly efficient, light-driven hydrogen evolution from water was demonstrated by using a poly(phenylene ethynylene) (PPE) bearing carboxylate-terminated Fréchet-type poly(benzyl ether) dendritic side groups, G1 to G3, as the photosensitizer.<sup>[37]</sup> Greater encapsulation of the conjugated backbone with increasing generation of dendritic appendages led to the suppression of undesirable self-quenching of the photoexcited state of PPE. Methylviologen ( $\text{MV}^{2+}$ ), a positively charged electron acceptor, was found to aggregate along the negatively charged surface of the dendronized PPE, thereby generating a spatially segregated donor-acceptor supramolecular complex (Figure 3). Time-resolved fluorescence spectroscopy showed that the fluorescence quenching rate constant for the third generation dendronized linear polymer ( $k_q = 1.2 \times 10^{15} \text{ M}^{-1} \text{ s}^{-1}$ ) was much greater than most diffusion-controlled rate constants, and was consistent with the high rate of electron transfer ( $k_{\text{ET}} = 9.3 \times 10^9 \text{ s}^{-1}$ ) afforded by the supramolecular assembly. Upon excitation of **8** in the presence of a mixture of  $\text{MV}^{2+}$ , triethanolamine (as a sacrificial electron donor), and colloidal PVA-Pt, hydrogen evolution took place with an overall efficiency of 13%, an order of magnitude better than prior systems based

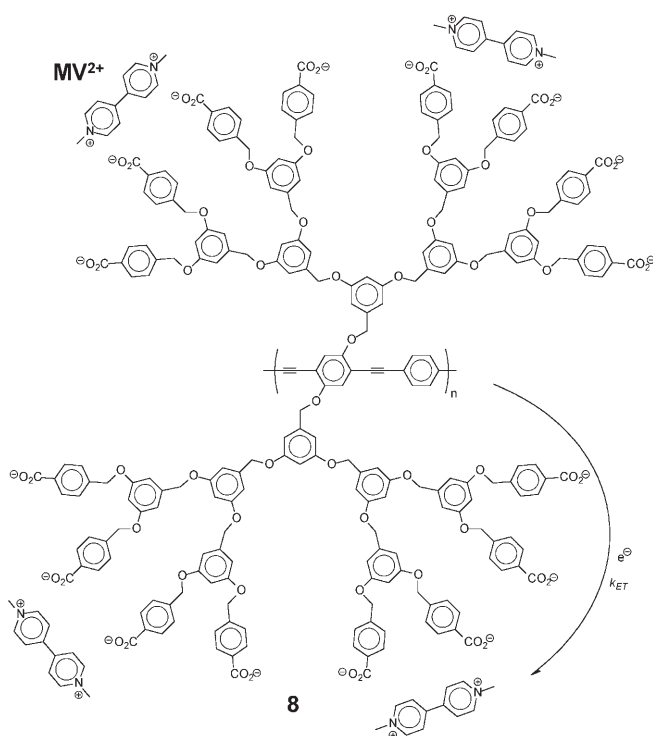


**Figure 3.** Carboxylate-terminated dendronized PPE with surface-bound methylviologens ( $MV^{2+}$ ) used in photodriven hydrogen evolution.

on common organic dyes. Comparative studies with several reference sensitizers suggest that spatial isolation of the conjugated backbone and its long-range  $\pi$ -electronic conjugation, along with electrostatic interactions on the exterior surface, play important roles in achieving such efficient photosensitized water reduction.

While many of the prominent features of site-isolation have thus far been described in detail, no particular mention has been made regarding the dielectric nature of the nanoenvironment generated by the dendritic polymer and how that might affect catalysis. Dielectric effects on catalytic reactions are well documented, as are microenvironment effects in catalysis applications involving soluble and insoluble polymer supports.<sup>[38]</sup> Certainly those exerted by a soluble polymer on the nanoscale should behave similarly. Piotti and co-workers reported an early example on the subject of nanoenvironment effects in catalysis with dendrimers. In this work, third and fourth generation unimolecular dendritic reverse micelles were prepared with a radial polarity gradient consisting of a non-polar corona resembling the reaction solvent and more polar ester or alcohol functionalities at pre-determined locations throughout the interior (Figure 4).<sup>[39]</sup> These dendrimers were specifically designed to catalyze reactions in which a nascent positive charge develops during the transition state: for

example, the simple unimolecular dehydrohalogenation of 2-iodo-2-methylheptane, which proceeds *via* an E1 elimination mechanism. Dendrimers with polyol interiors outperformed those with polyester cores. In addition, yields were significantly improved using the larger G4 dendrimer. One of the most striking features of this catalyst system was its ability to achieve high turnover even at very low catalyst loadings. Up to 99% conversion was observed in the elimination reaction using as little as 0.01 mol% of the G4 polyol-cored catalyst while no reaction was observed in control experiments without the dendrimer. The authors attributed this result to a kinetic but thermodynamically driven “concentrator effect” whereby the polarity gradient inherent to the dendrimer drives the relatively polar substrate into the macromolecule’s core leading to its accumulation in a constrained nanoenvironment that was more suitable for the E1 elimination than the external reaction medium, hexane. Higher generation dendrimers showed better efficacy for the reaction due to a larger internal reaction volume that could accommodate a higher concentration of substrate molecules. In addition, the non-polar alkene product had a greater affinity for the hydrophobic surrounding medium thereby achieving the necessary turnover. The authors have described this latter phenomenon as a free-energy driven “catalytic pump.”

These concepts, a “concentrator effect” to accumulate substrates near a catalytically active site and a “catalytic pump” to prevent product inhibition, have been broadly applied to other dendrimer catalysts with amphiphilic designs. Hecht and co-workers reported the first results on light-driven catalysis at the core of the dendrimers *via* photosensitization.<sup>[40]</sup> In their design, a  $^1O_2$ -sensitizing benzophenone core was incorporated into globular dendrimers having a radial polarity gradient consisting of a hydrophobic interior and a hydrophilic surface exposed to the polar solvent. The resulting nanoscale photoreactors were created and applied to the oxidation of cyclopentadiene (CP) with dioxygen (Scheme 5). The non-polar core was designed both to favor substrate accumulation of the CP substrate and to increase the lifetime of the photogenerated  $^1O_2$ . To complete the catalytic cycle, the *endo*-peroxide cycloadduct **9** derived from  $^1O_2$  and CP was reduced *in situ* with thiourea to *cis*-2-cyclopentene-1,4-diol. Since the diol product **10** had a greater affinity for the surrounding medium, vacant sites for other non-polar cyclopentadiene substrates were generated and a high rate of turnover was achieved. Indeed, the authors reported rapid conversions to **10** within 1 h using only 0.1 mol% of catalyst, although photobleaching of the dendrimer (approximately 10% over 1 h) and CP dimerization prevented a complete reaction. Significantly greater yields were obtained with increasingly larger dendrimer photoca-

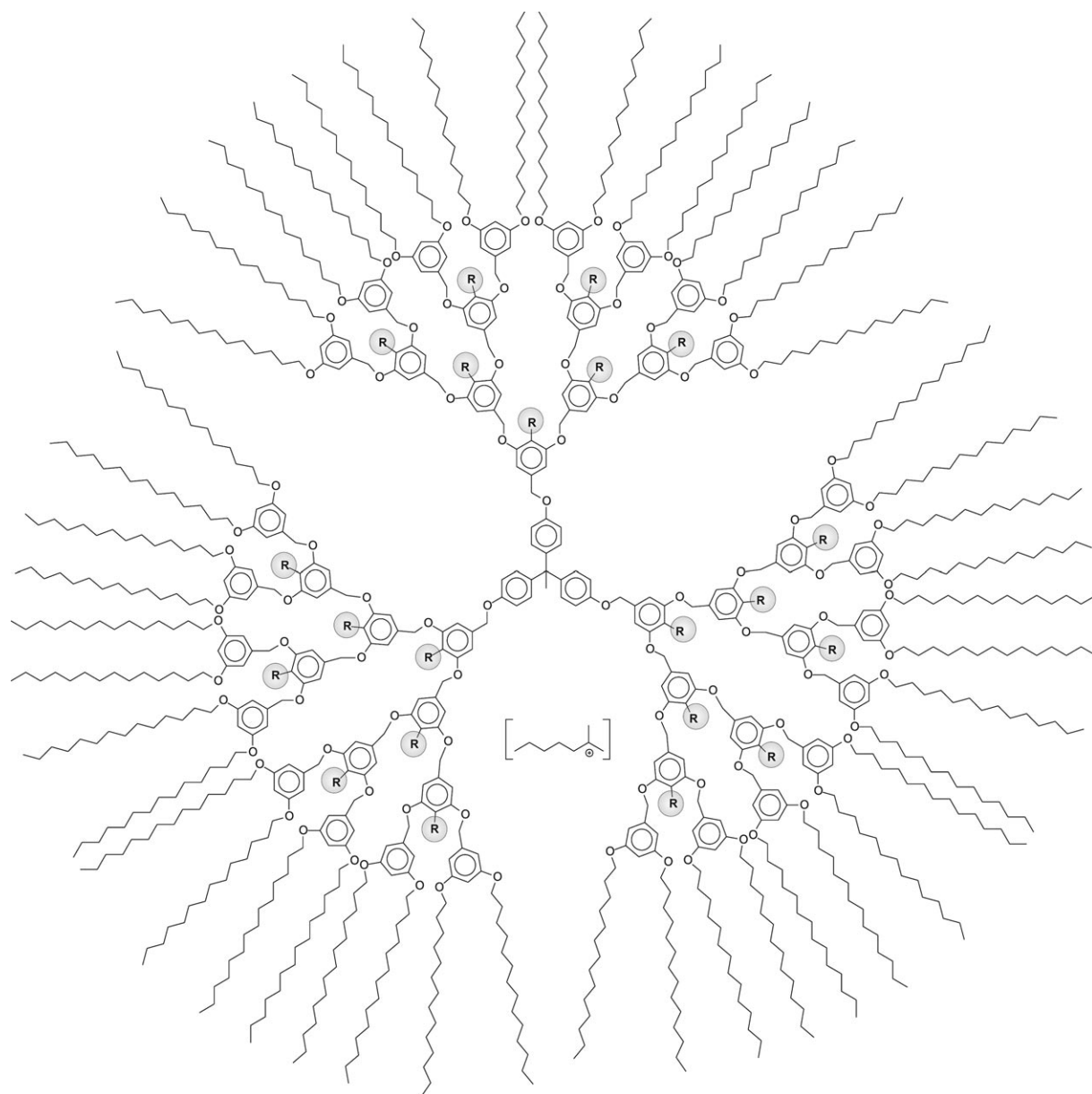


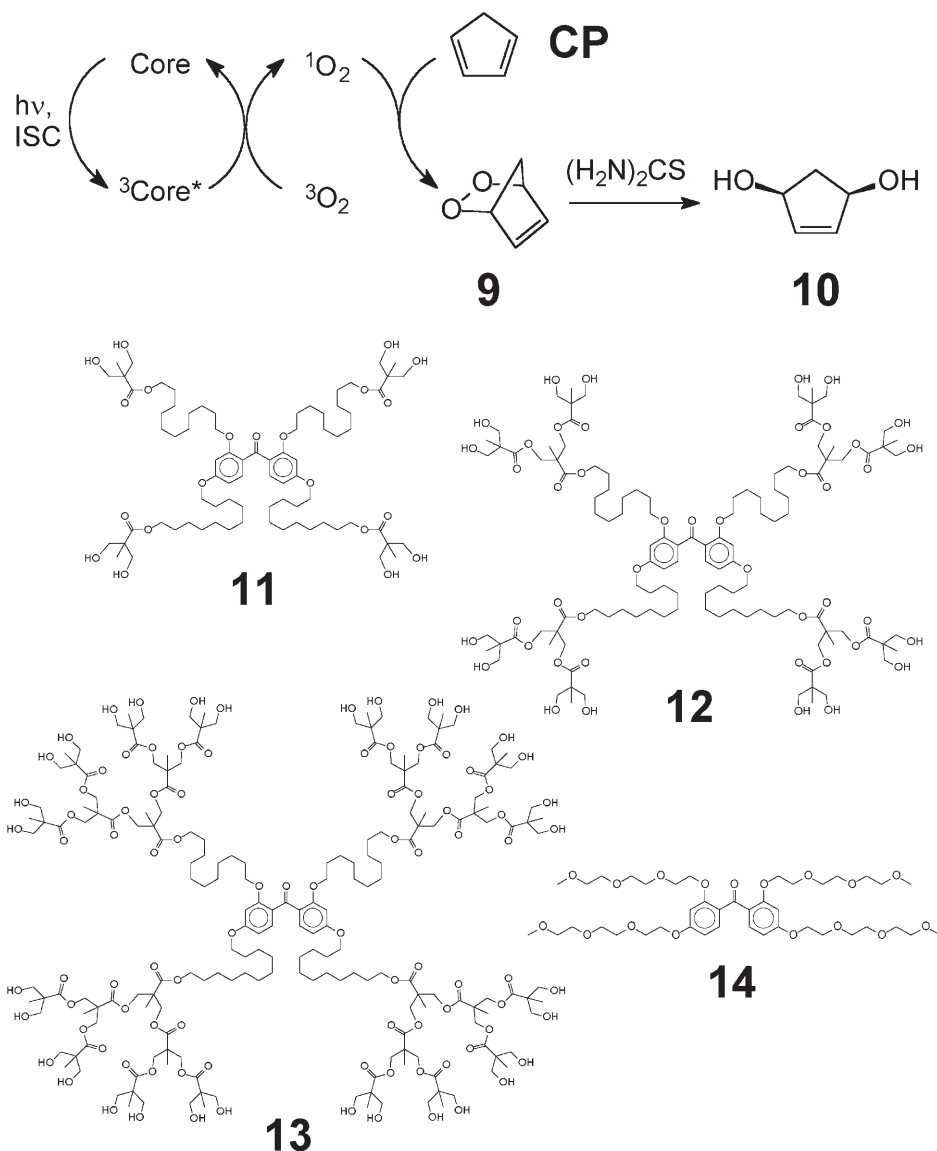
**Figure 4.** Fourth generation dendritic catalysts for E1 elimination reactions. Interior functionality:  $R = -\text{CO}_2\text{Me}$  or  $-\text{CH}_2\text{OH}$ .

talysts: G1 to G3 catalysts **11**, **12** and **13** gave the diol in overall yields of 15%, 35% and 50%. In contrast, a control experiment carried out using benzophenone model compound **14** with a hydrophilic triethylene glycol environment gave less than 10% of diol **10**. These data point to the importance of employing sufficiently large amphiphilic dendrimers with a hydrophobic interior to promote adequate substrate binding and accumulation at the site of reaction.

Exploiting the precise chemical synthesis designed for dendrimers, Mizugaki et al. were able to concentrate multiple functionalities at the cores of a series of amphiphilic dendrimer catalysts in order to determine the kinetic consequences of the steric shield at their apolar periphery. To that end, the periphery of

a third generation PPI dendrimer was functionalized with either  $\text{C}_{10}$  or  $\text{C}_{16}$  acyl chains. Their interiors were then quaternized with iodomethane to afford lipophilic tetraalkylammonium iodide dendrimers.<sup>[41]</sup> These dendrimers were used as Lewis base catalysts (*via* iodide ions) for the Mukaiyama aldol reaction of 1-methoxy-2-methyl-1-(trimethylsilyloxy)propene **15** with various aldehydes in toluene (Scheme 6). This study showed that dendritic iodides were remarkably more effective than other “small molecule” sources of iodide, such as tetrabutyl- or tetrahexylammonium salts. The authors argued that the higher activity of the dendrimers over the discrete small molecule iodides stemmed from the high polarity of the nanoenvironment encapsulating the iodide



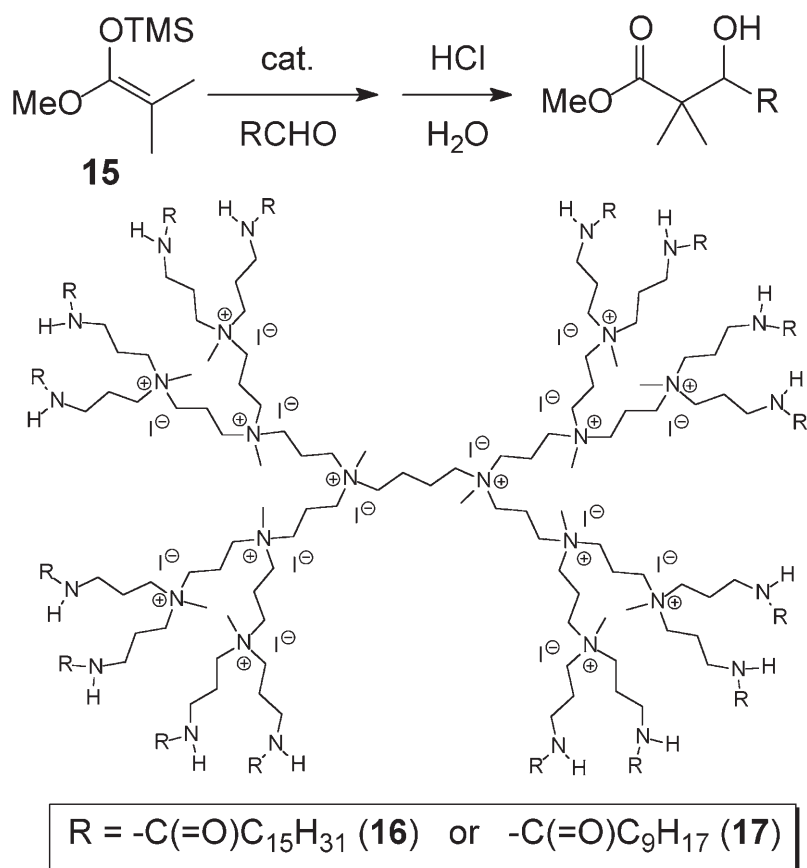


**Scheme 5.** Light-driven photooxidation of cyclopentadiene by dendritic benzophenone-cored  $^1\text{O}_2$  sensitizers.

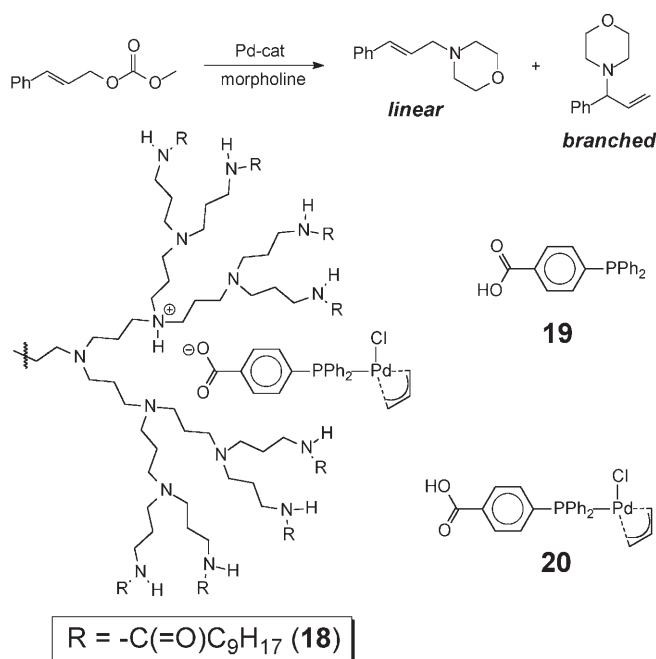
in the macromolecular catalysts. They noted that these reactions are promoted to a greater extent in polar solvents such as DMF as opposed to toluene. Thus, the concentration of multiple cationic charges within the nanoscopic confines of the dendritic interior appears uniquely capable of stabilizing the reactive anionic intermediate. In addition, a study of the steric effects showed that dendrimer **16** with a more crowded periphery (i.e., with  $\text{C}_{16}$  chains) did not perform as well as **17** with  $\text{C}_{10}$  peripheral chains. Therefore, the reaction of **15** with benzaldehyde in the presence of dendrimer **17** reached 98% yield of the silylated aldol while only 32% yield was obtained with dendrimer **16** under the same reaction conditions. This work clearly delineated the opportunistic design features of a dendritic catalyst concentrating reactive moieties within a small reaction volume at

the core of the dendrimer and using the dielectric constant of this discrete nanoenvironment to enhance reactivity, while stressing that sufficient access to that environment is also important.

The control of reaction selectivity through dielectric effects exerted by the dendrimer nanoenvironment has also been observed by Ooe and co-workers in Pd-catalyzed Heck reactions and allylic aminations. The catalysts were prepared using a self-assembly approach from decanoyl-terminated PPI dendrimers, G2 to G4, and 4-diphenylphosphinobenzoic acid as ligand for the metal center (Scheme 7).<sup>[42]</sup> The acid-amine ion pair ensured selective catalyst placement at the interior of the dendrimer. Subsequent treatment of the supramolecular construct with  $[\text{PdCl}(\text{C}_3\text{H}_5)]_2$  generated the active catalyst **18**. Testing of the catalysts in Heck reactions between iodobenzene and *n*-butyl ac-



**Scheme 6.** Dendritic tetraalkylammonium iodides as catalysts for the Mukaiyama aldol reaction of 1-methoxy-2-methyl-1-(trimethylsilyloxy)propene with various aldehydes.



**Scheme 7.** Pd-catalyzed allylic amination by dendrimer-bound Pd- $\pi$ -allyl complexes and model compounds.

rylate showed that the rate of reaction increased with increasing generation, while in the absence of the dendrimer no catalysis was observed. A similar reaction between 1,4-diiodobenzene and *n*-butyl acrylate with the G4 dendrimer catalyst proceeded with good selectivity for the mono-Heck adduct (*mono:di* = 92:8) while the catalyst system derived from only **19** showed little selectivity (*mono:di* = 45:55). These experiments strongly suggest that catalysis occurs *inside* the dendrimers.

In contrast to the rate acceleration with increasing generation seen for Heck reactions using self-assembled Pd-allyl complexes, the allylic amination reaction of cinnamyl methyl carbonate with morpholine catalyzed by the same catalysts showed decreasing activity with increasing dendrimer generation (Scheme 7). However, linear to branched ratios were higher for larger dendrimer catalysts (*l/b* = 9.1 for G4) and significantly higher than that for **20** (*l/b* = 5.1). It is known that solvent polarity affects *l/b* ratios, with the more polar solvents giving higher values (*l/b* = 14.1 in DMSO). Thus a significant nanoenvironment effect can be attributed to the polymer support in that the charged interior where the catalysts reside was responsible for the higher *l/b* ratios.

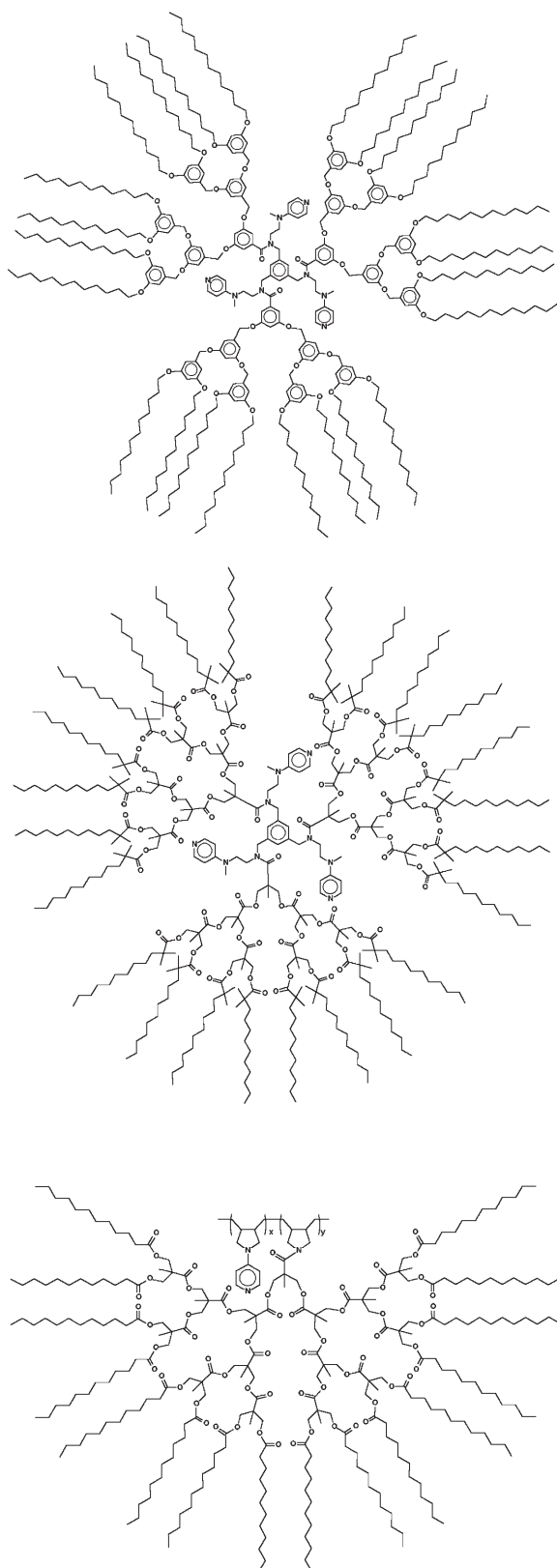


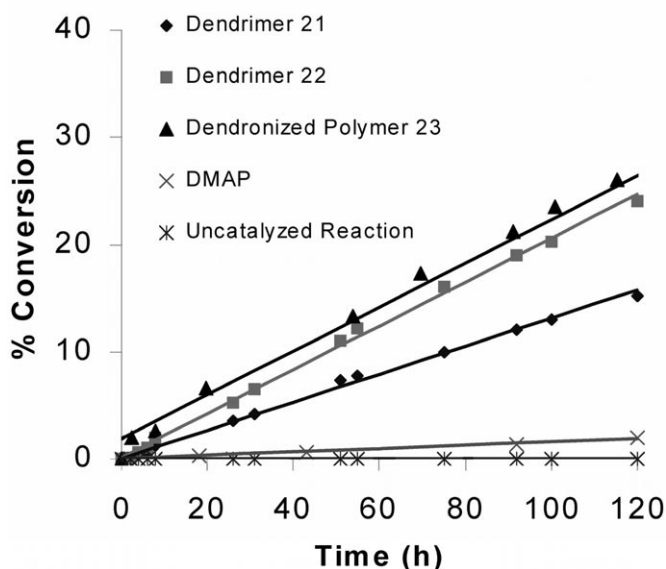
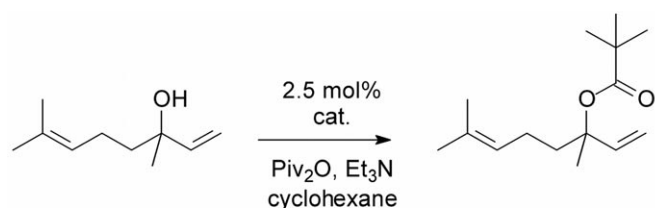
**Figure 5.** Dendritic 4-(dialkylamino)pyridine catalysts for acylation reactions.

21

22

23

The first systematic treatment of the specific roles of macromolecular architecture and nanoenvironment in the catalytic properties of dendritic polymers was reported by Helms and co-workers for a related pair of dendrimers and a dendronized linear polymer containing 4-(dialkylamino)pyridines.<sup>[43]</sup> The catalytic properties of these materials were investigated in the context of acylation reactions employing sterically demanding tertiary alcohols as substrates. Amphiphilic Fréchet-type benzyl ether and aliphatic ester G3 dendrimers **21** and **22**, respectively, were prepared from a common trivalent core containing three 4-(dimethylamino)pyridine (DMAP) analogues while a polyester dendronized linear polymer **23** containing 4-(pyrrolidino)pyridines (PPY) along the backbone was also prepared (Figure 5). Catalysis experiments clearly indicated that the nanoenvironment played the dominant role in determining the activity of the polymer catalysts, with the polyester platform being superior to the benzyl ether (Scheme 8). It was noteworthy that model compounds DMAP and PPY were only marginally effective for the transformation under the reaction conditions employed while the dendritic catalysts were more competent. These results were consistent with the “concentrator effect” previously described for amphiphilic dendrimers as the alcohol substrates partitioned preferentially into the more polar core of the dendrimers from the non-polar reaction



**Scheme 8.** Formation of linalool pivalate with time for various 4-(dialkylamino)pyridine catalysts.

medium (i.e., cyclohexane). As a result, the reaction benefited from a higher local concentration of substrate near the catalyst thereby affecting the rate. In addition, the non-polar ester product of the reaction likely diffused back into the solvent to minimize free energy thus giving rise to a “catalytic pump” to achieve turnover. Interestingly, polymer architecture played little or no role in affecting rates of catalysis as both the dendrimer and the dendronized linear polymer based on the same polyester platform showed comparable reaction kinetics. With respect to molecular transport and catalysis, this represented the first comparative study of the effect of architecture and nanoenvironment using structurally similar dendritic materials. Other work has appeared in the literature further documenting this effect with Ru-BINAP dendrimers and dendronized linear polymers.<sup>[44]</sup>

Another salient feature of dendrimers bearing one or more catalytically active sites at their core is their ability to achieve substrate selectivity through steric restriction. In the literature, this has often been referred to as “shape selectivity.” The pioneering work with shape selective catalysts was performed by Bhayappa et al. with dendritic manganese porphyrins.<sup>[45]</sup> This was followed by several reports by Crooks and co-workers using dendrimer encapsulated nanoparticles.<sup>[46]</sup> In all of these reports is a common thread that relates substrate flexibility to its interaction with the polymer catalyst and the kinetic ramifications that derive from such an interaction. In more recent work, the kinetic behavior of various guest molecules with different steric constraints was investigated using distance-dependent excited state quenching through photoinduced electron transfer.<sup>[47]</sup> Anthracene-cored dendrimers were prepared from Fréchet-type dendrons up to the fourth generation (Figure 6). Core accessibility was probed using trialkylamines, which are known to quench the photoexcited state of the anthracene chromophore through electron transfer. Various trialkylamines of different sizes and rotational degrees of freedom were used as quenchers, including triethylamine ( $\text{Et}_3\text{N}$ ),  $N,N,N',N'$ -tetramethylethylenediamine (TMEDA),  $N,N,N',N',N'',N''$ -hexamethyltris(2-aminoethyl)amine (TREN- $\text{Me}_6$ ), diazabicyclooctane (DABCO), and  $N,N$ -dimethylaminoadamantane (ADM- $\text{NMe}_2$ ). Each of these amine-based quenchers gave smaller Stern–Volmer bimolecular quenching rate constants,  $k_q$ , with increasing dendrimer generation; for example,  $k_q$  values for  $\text{Et}_3\text{N}$  were  $3.5$ ,  $3.2$ ,  $2.9$  and  $2.0 \times 10^9 \text{ M}^{-1} \text{ s}^{-1}$  for the G1 to the G4 anthracene-cored dendrimers. This is consistent with the greater site isolation achieved with the increasing larger dendritic shells at higher generations. In addition, geometrically constrained molecules were found to have better access to the dendrimer cores than their more flexible counterparts. For example, TMEDA ( $\text{C}_6\text{H}_{16}\text{N}_2$ ) and DABCO ( $\text{C}_6\text{H}_{12}\text{N}_2$ ) were

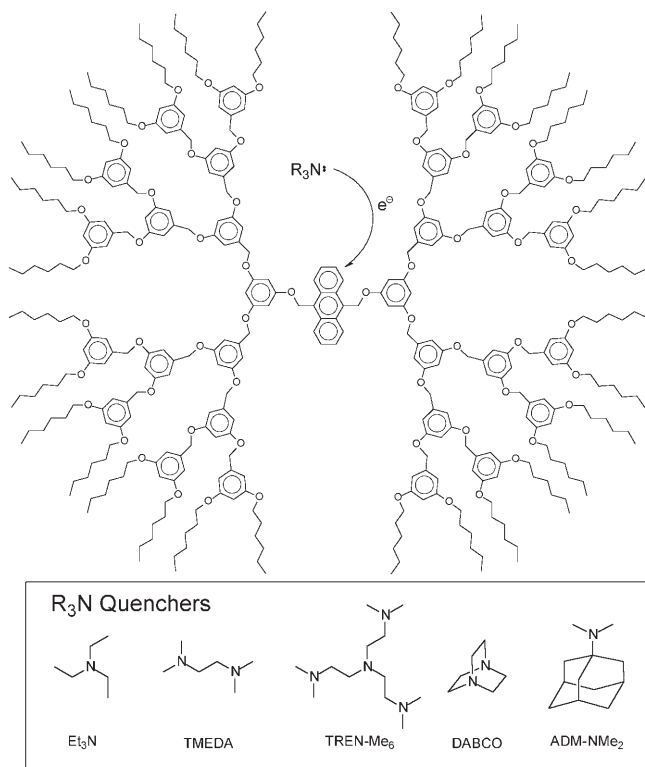
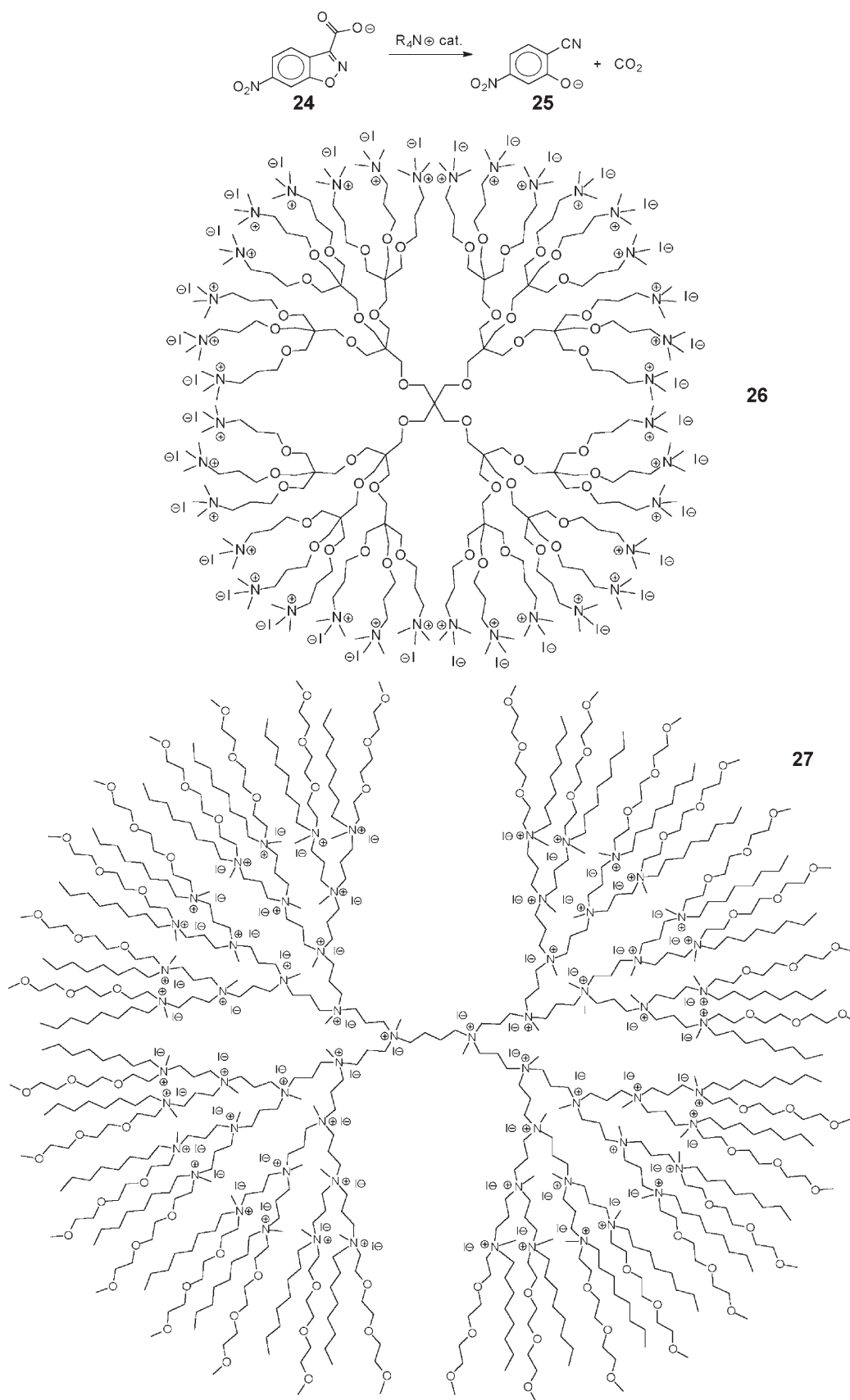


**Figure 6.** Quenching of photoexcited anthracene at the cores of dendrimers by various amines.

used in this comparative study given their similar molecular composition but different geometry. The quenching constants measured for the G4 dendrimer were  $k_q = 1.7 \times 10^9 \text{ M}^{-1} \text{ s}^{-1}$  for TMEDA and  $k_q = 11.3 \times 10^9 \text{ M}^{-1} \text{ s}^{-1}$  for DABCO, indicating that the more rigid DABCO can reach the core more easily than its more flexible counterpart TMEDA. These results are consistent with other reports in the literature and provide fascinating insight into the shape selectivity for substrates using dendritic catalysts.

The placement of catalytic groups at the periphery or within the interior of a dendrimer obviously has a great effect on the outcome of reactions using dendrimer catalysts. In a thorough related body of work from the Ford group, the effect of dendritic quaternary ammonium salts on the unimolecular decarboxylation of 6-nitrobenzisoxazole-3-carboxylate **24** was investigated using dendrimers with either peripheral or internal functionalization (Scheme 9). The peripherally modified dendrimer **26** was prepared by exhaustive methylation of a second generation polyether dendrimer with 36 primary amine groups at its surface.<sup>[48]</sup> While the binding constant of **24** with **26** compares favorably with those measured for analogous micelles, various polyelectrolytes and even latices, the observed rate constant for decarboxylation of **24** at  $[\mathbf{24}]_0 < 10^{-4} \text{ M}$  was only 20 times faster in the presence of  $< 1.0 \text{ mg mL}^{-1}$  of **26** than in water alone (i.e.,  $k_{\text{cat}}$





**Scheme 9.** Decarboxylation of 6-nitrobenzoxazole-3-carboxylate using dendritic quaternary amines either located at the periphery or alternatively within the interior of the polymer.



**Scheme 10.** Transaminase activity by dendrimer-bound pyridoxamines (G6 dendrimer shown) to pyruvic acid derivatives.

$k_{\text{water}}=20$ ) whereas those for other systems typically fall in the range of  $k_{\text{cat}}/k_{\text{water}}=150\text{--}9,000$  for micelles and even higher in the latices [ $k_{\text{cat}}/k_{\text{water}} > 21,000$  for a lipophilic poly[(styrylmethyl)tributylammonium] ion latex]. Thus, while the dendrimer did provide a suitable motif for substrate binding, the solvent-exposed environment of its surface was too hydrated to destabilize carboxylate **24** for subsequent reaction.

In later work, the Ford group employed fully quarternized PPI dendrimers of generations 2 to 4 in which the primary amine periphery had been functionalized with both  $\text{C}_8$  alkyl chains and triethylene glycol monomethyl ethers to impart some hydrophobicity to the substrate-binding interface while maintaining aqueous solubility (Scheme 9).<sup>[49]</sup> These catalysts showed marked improvement over the previously studied hydrophilic dendrimers with structure **26**. For example, the second and fourth generation dendrimers gave  $k_{\text{cat}}/k_{\text{water}}$  values of 323 and 564, respectively. In addition, binding constants were shown to increase with increasing dendrimer generation, suggesting a synergistic positive dendrimer effect. While these materials reached an activity that was on par with micellar systems, they did not outperform conventional ion latices in this reaction. However, the study clearly illustrates the importance of functional group placement in the framework of a dendritic catalyst and its effect on the catalytic activity.

Core-modified dendrimers have also been used as biomimics. Polymers bearing pyridoxamines<sup>[50,51]</sup> and pyridoxals<sup>[52]</sup> have some success as mimics of transaminases and amino acid racemases, respectively, as reported by Breslow's group. Building on their previous work with functionalized polyethylene imine linear polymers, a series of PAMAM dendrimers were prepared with either of the active residues at their core. For the sake of both clarity and brevity, this review will only focus on the positive dendrimer effects afforded by the pyridoxamine PAMAM dendrimers, G1 to G6, in the transamination of pyruvic acid and phenylpyruvic acid in aqueous buffer (Scheme 10).<sup>[53]</sup> The pyridoxamine PAMAM dendrimers displayed Michaelis–Menten kinetics and superior efficacy when compared to the simple pyridoxamine. Interesting positive dendrimer effects were drawn from the observed Michaelis–Menten parameters – i.e., the second order rate constant  $k_2$ , the binding constant  $K_M$ , and the ratio  $k_2/K_M$  – as they changed with increasing generation. The larger dendrimers were much more efficient at facilitating general acid-base reactions along the catalytic pathway leading to a net increase of  $k_2$ . In the case of the transamination reaction of pyruvic acid, the G3 PAMAM catalyst gave  $k_2=66\times 10^3\text{ min}^{-1}$  while the corresponding G6 gave a  $k_2$  value of  $180\times 10^3\text{ min}^{-1}$ . Through structural variants, the authors showed that this effect was in large part due to the tertiary amines

that reside at the periphery of the dendrimers. In addition, this series of dendrimers showed enhanced substrate binding as the globularity of the dendrimer increased. This effect was most pronounced when the substrate binding ability of the more hydrophobic phenylpyruvic acid was compared for different dendrimer generations. Therefore,  $K_M$  values for the G2 and G6 PAMAM dendrimers were 110 mM and 39 mM, respectively, with pyruvic acid as the substrate while they were 30 mM and 2.7 mM, respectively, with phenylpyruvic acid. These data, taken together, paint an interesting portrait of dendrimer activity for these pyridoxamine-cored PAMAM dendrimers: (i) the substrate binding ability of the dendrimers was improved as a more globular, enzyme-like conformation is reached at higher generations; (ii) better binding is achieved with a more hydrophobic substrate, although rates of reaction are comparable with those achieved with the more polar substrate; (iii) increasing the dendrimer generation leads to increases in reaction rates due to general acid-base catalysis that is a direct result of increasingly more tertiary amines at the periphery of the dendrimers.

## 4 Peripherally Modified Dendrimers in Catalysis

Peripheral modification of dendritic supports for catalysis offers unprecedented opportunity for active site multivalency and thus high loading capacity. In addition, the support often imparts other features that affect catalysis: unique solubility properties, proximal interactions between catalytic groups leading to cooperative effects or steric crowding at the periphery leading to a certain selectivity profile. All of these features are illustrated in the following examples that highlight positive dendrimer effects in peripherally modified dendrimers.

Metallocene catalysts find widespread use in the polymerization of  $\alpha$ -olefins.<sup>[54]</sup> The active form of the catalyst is cationic and is typically generated by a co-catalyst. Industrially, this is usually methylaluminumoxane (MAO) – a complex condensate derived from water and  $\text{AlMe}_3$  – or perfluorophenylborane,  $\text{B}(\text{C}_6\text{F}_5)_3$ . The interaction between the ion pair affects the overall activity, stereoregularity, chain transfer, termination rate and lifetime of the metallocene catalyst. Less nucleophilic counterions are particularly desirable; this has, in the past, been achieved through charge delocalization or steric shielding. However, in their work, Mager and co-workers achieved this through steric crowding at the surface of a peripherally modified carbosilane dendrimer.<sup>[55]</sup> Co-catalysts G0 to G2 were synthesized with 4, 12, and 36 alkyl-tris-(pentafluorophenyl)borates at the periphery

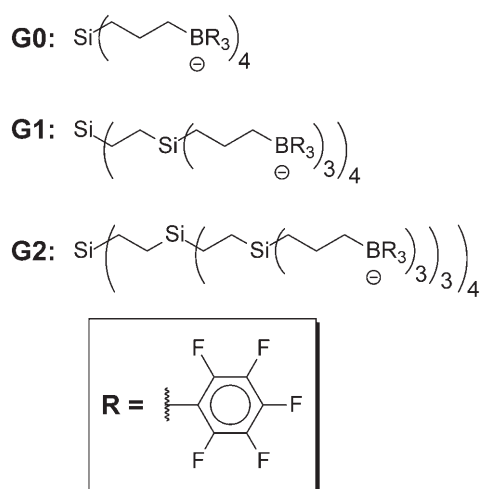


**Figure 7.** Dendritic polyanions for  $\alpha$ -olefin polymerization co-catalysts.

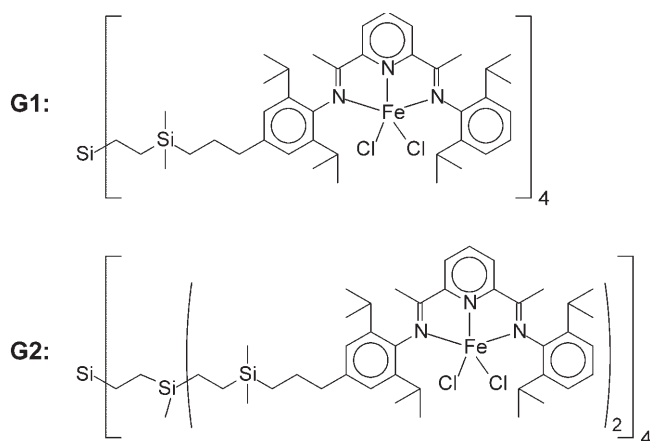


**Figure 8.** Dendritic bis(imino)pyridyl-Fe(II) complexes for  $\alpha$ -olefin polymerization.

(Figure 7). When employed with  $[(\text{Ind})_2\text{ZrMe}_2]$  metallocene co-catalysts, these non-coordinating dendrimer polyanions were highly active in ethylene polymerization and copolymerizations with propylene or 1-hexene, although activity was not generation-dependent. Unlike non-coordinating small molecule anions resulting from  $\text{B}(\text{C}_6\text{F}_5)_3$ , the dendrimer polyanions gave high activities even in aliphatic solvents, with no apparent loss in activity at reaction times greater than 40 min. This positive dendrimer effect was thought to arise from the specific and unique interaction between the active cationic metallocene co-catalyst and the crowded anionic surface of the dendrimer.

In a similar study relating the nature of the interaction between a dendritic polymerization catalyst with a conventional anionic co-catalyst, Zheng and co-workers prepared first and second generation carbosilane metallodendrimers bearing bis(imino)pyridyl iron(II) catalyst precursors at their periphery

(Figure 8).<sup>[56]</sup> After activation with modified methylaluminumoxane (*m*-MAO) at a ratio of  $\text{Al/Fe} > 1200$ , the rate of ethylene polymerization for either of the multivalent dendrimer catalysts was comparable to the parent Fe catalyst. However, at lower Al/Fe ratios ( $< 1000$ ), the activities of both dendrimer catalysts were superior to the small molecule catalyst. For example, at an Al/Fe ratio of 500, a typical polymerization with the small molecule bis(imino)pyridyl iron(II) catalyst, the first generation catalyst bearing four groups, and the second generation bearing eight groups, the activities measured were 1.14, 2.52 and  $2.54 \times 10^3 \text{ kg PE mol}_{\text{Fe}}^{-1} \text{ h}^{-1}$  demonstrating the higher efficacy of the dendritic platform. In addition, the molecular weight and the melting temperature ( $T_m$ ) of the polyethylene obtained increased with the generation of the dendrimer catalyst:  $T_m = 127.9$ , 133.9 and  $134.1^\circ\text{C}$  for the parent, G1 and G2 catalysts, respectively. Again, this positive dendrimer effect was generally thought to involve a fundamentally different interaction of the dendritic periphery with the polymeric counterion derived from *m*-MAO than was experienced with the small molecule catalyst system.

While the previous examples focused on catalyst systems that generated linear PE, catalysts that give rise to branched polyethylene through a chain walking mechanism are also well known.<sup>[57]</sup> Late transition metal polymerization catalysts, including the Ni(II) N/N pyridylimine type, generate ethylene derivatives ranging from light oligomers to high molecular weight polymers with varying degrees of branching.<sup>[58]</sup> Varying reaction conditions or tuning ancillary ligands can generate selectivity profiles for molecular weight and/or degree of branching. It was thought that unique selectivity characteristics might also arise from catalyst confinement at the dendritic periphery. Using the aforementioned Ni(II) catalyst system, the groups of de Jesús and Flores synthesized a series of carbosilane dendrimers, G0 to G3, with 1, 4, 8 and 16 Ni(II) pyridylimines, respectively (Figure 9).<sup>[59]</sup> They reported a strong generation dependence on the molecular weight and topology of the final product mixture: a toluene-soluble fraction comprised of  $\alpha$ -olefin oligomers and an insoluble high MW PE fraction. With increasing generation of the dendrimer catalysts, there was a stronger preference for oligomerization, and hence chain transfer, over polymerization. For example, the oligomerization activities for G0 to G3 were measured at 5.2, 8.3, 10.2 and  $13.4 \text{ g mol}_{\text{Ni}}^{-1} \text{ h}^{-1} \text{ bar}^{-1}$ , while a concomitant decrease in polymerization activity was observed. The oligomer fraction showed Schulz–Flory chain length distributions,  $\alpha$ , that decreased with increasing nuclearity (e.g.,  $\alpha_{\text{G0}} = 0.70$  while  $\alpha_{\text{G3}} = 0.45$ ). Surface confinement of the catalysts on dendrimers also affected the topology of the toluene-insoluble polymer fraction. Significantly less branched and higher MW PE was observed with the



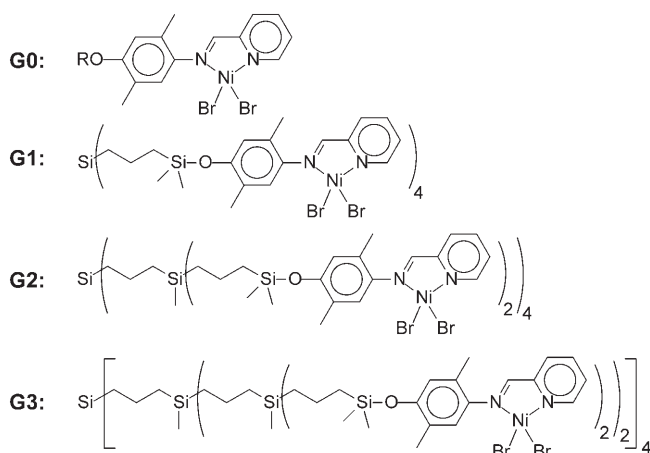
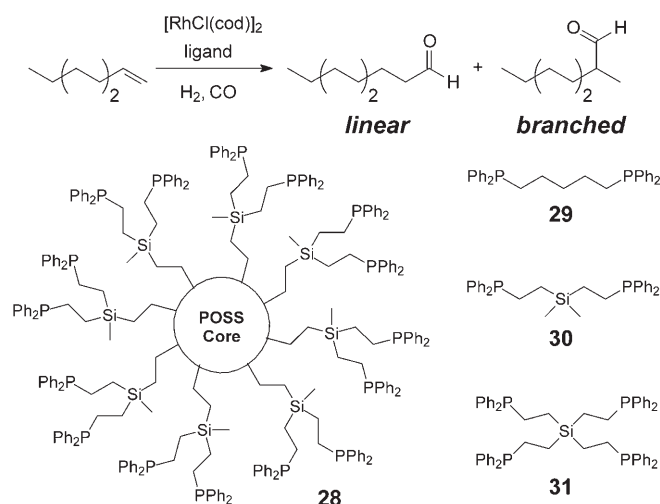


**Figure 9.** Dendritic iminopyridyl-Ni(II) chain-walking polymerization catalysts for  $\alpha$ -olefin polymerization.

larger dendrimers. Thus, the chain-walking ability of the polymer-bound catalysts appears to be affected by congestion at the periphery and the metal centers at the periphery were more protected thus giving rise to higher MWs. Whether or not this constitutes a positive dendrimer effect is debatable, however, it does provide another example of how polymerization events are modulated by catalysts restricted in location at the dendritic periphery.

High selectivities for linear over branched isomers for reactions involving alkenes at transition metal sites located at the periphery of a dendrimer have also been observed in the Rh(I)-catalyzed hydroformylation reaction using diphenylphosphine-functionalized polyhedral oligomeric silsesquioxane (POSS) dendrimers as ligands (Scheme 11).<sup>[60]</sup> During the hydroformylation of 1-octene, the catalyst derived from  $[\text{RhCl}(\text{cod})]_2$  and dendritic ligand **28** with 16 phosphines at its periphery showed unexpectedly high regioselectivity for the linear aldehyde nonanal ( $l/b = 14$ ). In comparative studies, small molecule analogues, including 1,5-bis(diphenylphosphino)pentane (**29**),  $\text{Me}_2\text{Si}(\text{CH}_2\text{CH}_2\text{PPh}_2)_2$  (**30**) and  $\text{Si}(\text{CH}_2\text{CH}_2\text{PPh}_2)_4$  (**31**), gave significantly lower selectivities ( $l/b = 3.4$ , 3.8 and 5.2, respectively) thus confirming the unusual selectivity of these dendritic ligands *via* a positive dendrimer effect. In this case, steric crowding at the dendritic periphery is thought to promote bidentate binding of adjacent phosphines to the rhodium(I) metal center, producing a ligand environment similar to large bite angle bidentate phosphine ligands, such as Xantphos and bis(diphenylphosphinomethyl)biphenyl, that also incur high regioselectivity in favor of the linear isomer.

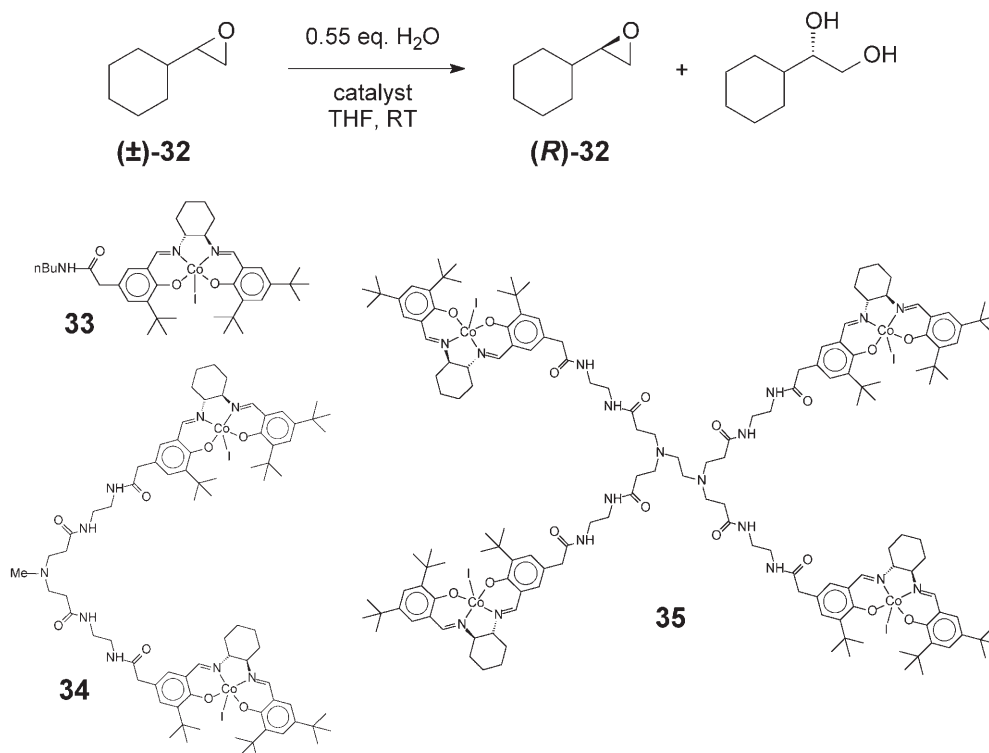
Reactions involving the co-operative interaction of multiple catalysts species have, in the past, been shown to benefit from their tethering, or covalent attachment through a linker. Catalyst tethering provides



**Scheme 11.** Hydroformylation of 1-octene using various Rh(I) catalysts derived from either dendritic or small molecule bisphosphines.

a useful tool for achieving high local concentrations of the complementary species in solution. Similar benefits may be derived from catalyst immobilization on the surface of dendritic supports. For example, the process of hydrolytic kinetic resolution (HKR) of terminal epoxides using cobalt(salen) complexes is thought to proceed *via* both substrate and nucleophile activation by two different metal-salen units. It was hypothesized that dendrimeric confinement of the Co-salen complexes at the surface of the macromolecule would reinforce cooperative catalytic activity. The HKR activity for  $(\pm)$ -**32** using PAMAM dendrimers G1 to G3 with 4, 8 and 16 residues at the periphery were measured and compared to the untethered catalyst and a dimer analog (Scheme 12).<sup>[61]</sup> Each of the dendrimers outperformed the model compounds **33** and **34**, indicating a positive dendrimer effect. However, the reaction rate was optimal at G1 (**35**) where only four catalyst molecules were conjugated to the support. Thus, a particular molecular geometry appears to be required for the HKR reaction and for this series of macromolecules was best obtained at G1.

With peripherally modified dendrimers, the dendrimer effect as expressed in greater than statistical improvement with increased catalyst nuclearity does not have to involve steric crowding or cooperativity between neighboring sites. For example, a large dendrimer effect was observed in the bromination of cyclohexene with hydrogen peroxide and NaBr catalyzed by a series of organochalcogenide Fréchet-type dendrimers with terminal  $-\text{O}(\text{CH}_2)_3\text{SePh}$  groups.<sup>[62]</sup> The catalytic cycle is thought to proceed *via* activation of the terminal phenyl selenides with  $\text{H}_2\text{O}_2$ , followed by hydration of the selenoxide to the dihydroxyselenane,



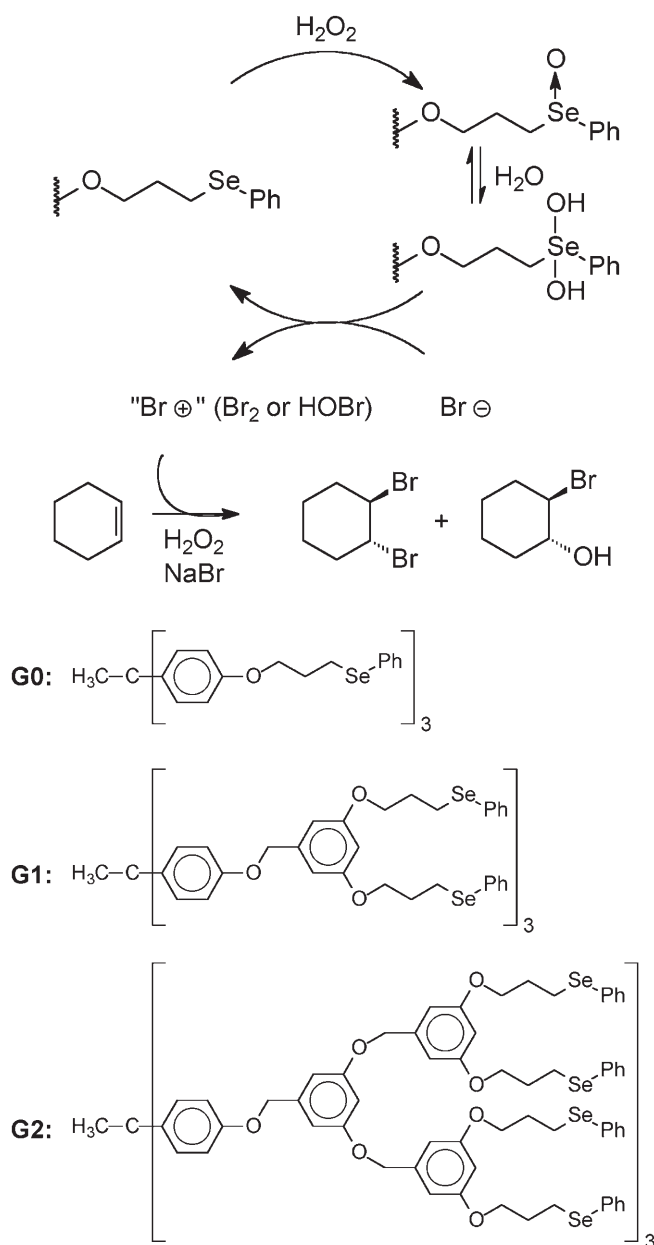
**Scheme 12.** Hydrolytic kinetic resolution of (*rac*)-vinylcyclohexane epoxide using Co-(salen) catalysts.

ligand exchange with  $\text{Br}^-$ , then reductive elimination of “ $\text{Br}^+$ ” (as  $\text{Br}_2$  or  $\text{BrOH}$ ) to complete the catalytic cycle (Scheme 13). Cyclohexene then traps the electrophilic bromine oxidant to give either *anti*-1,2-dibromocyclohexane or *anti*-2-bromocyclohexanol. Detty and co-workers observed an induction period for the oxidation of bromide anion with  $\text{H}_2\text{O}_2$  using the selenide-bearing dendrimers as catalysts. In contrast, addition of pre-formed dendritic selenoxide catalysts [i.e.,  $\text{R-Se(=O)Ph}$ ] gave rapid catalysis without an induction period. However, the authors report that the rates of oxidation of the selenides with  $\text{H}_2\text{O}_2$  under homogeneous or biphasic conditions, or even with *t*-BuOOH under homogeneous conditions, were too slow to account for the observed dendrimer effect on cyclohexene oxidation, especially since selenide oxidation rates were generally invariant between generations. Therefore, the large dendrimer effect in this system could not be explained by differences in the rates of oxidation at the dendrimer periphery.

The same study provided evidence of a slow background reaction between  $\text{Br}^-$  and  $\text{H}_2\text{O}_2$  that was capable of producing electrophilic bromine oxidants. These were then responsible for selenide oxidation at the dendrimer periphery, thus explaining the induction period. The process becomes autocatalytic as selenoxide formation accompanies further consumption of peroxide to form additional bromine oxidants (Figure 10). It must be noted that the rate of forma-

tion of “ $\text{Br}^+$ ” increased with increasing reaction time only in the case of the dendrimers. The reason for this lay in the localization of selenide pre-catalysts at the surface of the dendrimer. When “ $\text{Br}^+$ ” oxidizes one selenide at the dendrimer surface, it produces more “ $\text{Br}^+$ ” in close proximity to other selenides, which then undergo oxidation to the catalytically active selenoxides until the entire dendrimer surface has been activated. This dendrimer effect, due to autocatalysis, is strongest with the larger dendrimers because of the ability of the polymer to concentrate more pre-catalysts within the nanoscopic reaction volume.

Combinatorial approaches have also yielded well-defined dendritic catalysts with active catalyst species at their periphery. Reymond and co-workers have described a series of peptide-based dendrimers that are models for lipases.<sup>[63]</sup> These dendrimers are prepared using solid-phase synthesis with various diamino acid branching units that afford a dendritic architecture. Initial work sought to incorporate the catalytic triad of amino acids present in serine proteases in a combinatorial manner at various locations throughout the dendrimer in order to determine which spatial arrangement of reactive groups would be required for high activity and binding.<sup>[64]</sup> Some of the dendrimers in the library displayed remarkable esterolytic activity, even surpassing the activity of 4-methylimidazole as a model single-site small molecule catalyst, with a surprising degree of selectivity (Figure 11). For exam-



**Scheme 13.** Oxidation of cyclohexene using  $\text{H}_2\text{O}_2$  and NaBr in the presence of organoselenide dendritic catalysts.

ple, aspartate-terminated dendrimer **36** with internal histidine residues was selective for cationic 7-hydroxy-*N*-methylquinolinium ester substrates (**38–40**) while histidine-terminated dendrimer **37** was selective for anionic 8-hydroxypyrene 1,3,6-trisulfonate esters (Scheme 14). This behavior was explained on the basis of ion pairing. In addition, more lipophilic esters were found to be better substrates; interestingly,  $K_M$  values decreased with increasing acyl chain length for **38** to **40** or **42** to **45** while  $k_{cat}$  values remained essentially unchanged. Chiral discrimination was also observed for 2-phenylpropionate 7-hydroxy-*N*-methylquinolinium esters ( $\pm$ )-**41** with aspartate-terminated

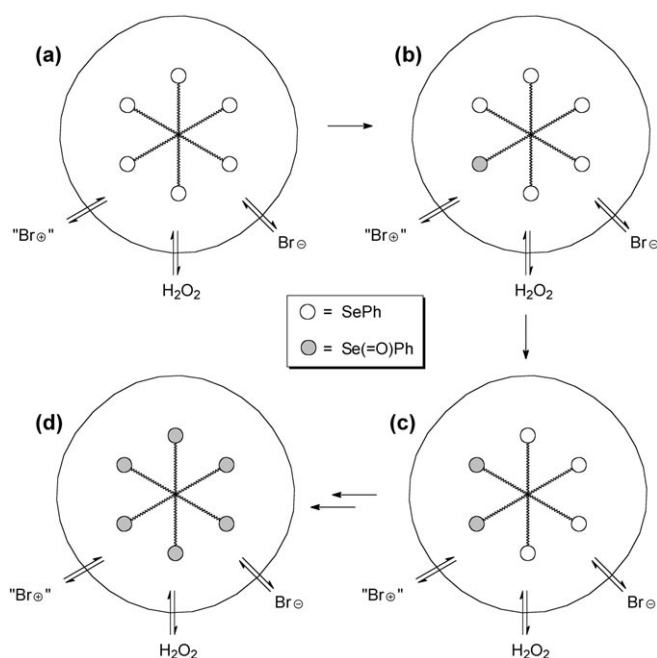


**Figure 10.** Autocatalytic activation of organoselenide dendrimers: (a) slow diffusion of “ $\text{Br}^+$ ” near the dendrimer; (b) activation of  $-\text{SePh}$  by “ $\text{Br}^+$ ”; (c) selenoxide formation results in “ $\text{Br}^{++}$ ” production which further activates more  $-\text{SePh}$  groups (autocatalysis); and (d) complete activation of the dendrimer surface.

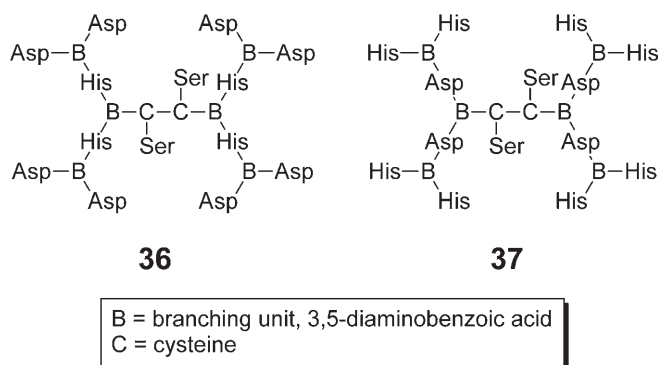
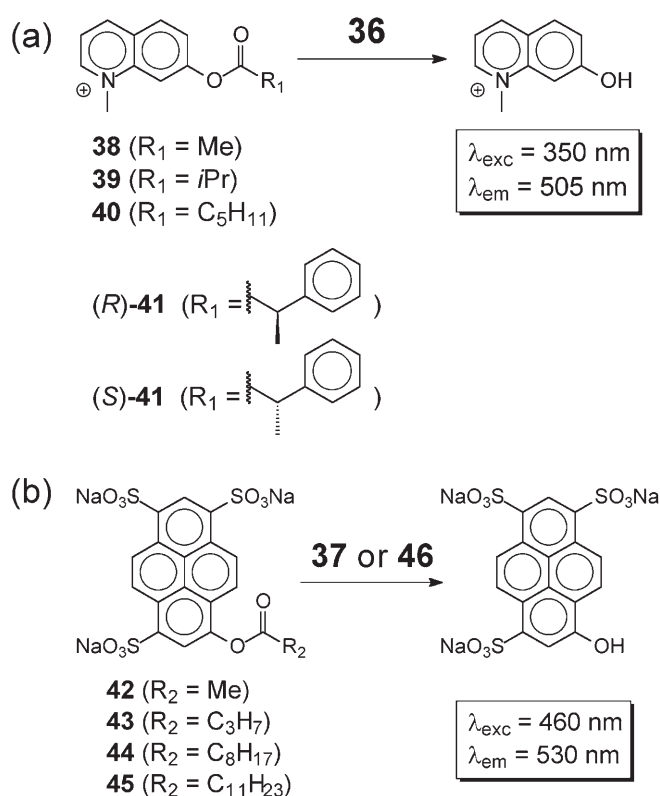


**Figure 11.** Aspartate- and histidine-terminated dendrimers – **36** and **37**, respectively – for catalytic and selective esterolysis.

dendrimer **36** containing the polyhistidine cores. Again,  $k_{cat}$  values for both enantiomers of **40** were similar, while a lower  $K_M$  value was observed for the (*S*)-enantiomer. Finally, the authors were able to show that a single His to Ala substitution in **37** led to a 75 % loss of catalytic activity suggesting that a cooperative mechanism requiring at least two His residues at the periphery is involved. In these examples, the dendrimer effect arises from the ability to precisely place various functional groups at specific locations throughout the structure of the dendrimer.



**Scheme 14.** Selective ester hydrolysis by peptide dendrimer catalysts: (a) cationic quinolinium esters as substrates; (b) anionic hydroxypyrene trisulfonate ester substrates.

In a more recent report,<sup>[65]</sup> the presence of a strong positive dendrimer effect with increasing generation of peptide-dendrimer catalyst was quantified using a series of dendrimers G1 to G4 whose catalytically active repeat unit was a His-Ser dipeptide while 2,3-diaminopropanoic acid afforded the branching (Figure 12). Michaelis–Menten parameters for the macromolecular catalysts were measured at each dendrimer generation. When selectivity constants,  $k_{\text{cat}}/K_M$ , were normalized to the background rate of reaction,  $k_2$ , obtained using 4-methylimidazole as a control and subsequently normalized to the number of histidines in the catalyst structure (i.e.,  $k_{\text{cat}}/K_M/k_2/\text{His}$ ), a non-linear increase in histidine reactivity reaching a factor of 100 was observed with increasing generation of the dendrimer from G1 to G4. Isothermal titration calorimetry was used to determine the association constants and the number of binding sites for a slow reacting substrate (**45**) and the hydroxypyrene trisulfonate product. Not surprisingly, larger dendrimers were able to bind more substrate molecules: for example, while G1 and G2 dendrimers only show approximately 2 binding sites, 10 binding sites are observed for G4. Larger association constants for substrate **45** were observed with increasing dendrimer generation:  $K_a = 1.66, 10.5, 56.2$  and  $80.8 \times 10^4 \text{ M}^{-1}$  for the series of peptide-dendrimer catalysts G1 to G4.

Interestingly, all of the dendrimers displayed similar yet markedly weaker association constants for the hydrolyzed product ( $K_a = 0.11\text{--}0.28 \times 10^4 \text{ M}^{-1}$ ). High rates of turnover were ensured, especially with the largest dendrimers, as substrate binding was two orders of magnitude higher than that for the product. Thus, the strong positive dendrimer effect in this system can be attributed to both the enhanced substrate binding and the greater contribution of the proximal histidine residues to the overall rate of catalysis (Figure 13).

## 5 Conclusion and Outlook

The dendrimer effect – that is, the advantages associated with catalyst immobilization onto dendrimer supports – appears to have a very broad scope. For core-functionalized dendrimers, this effect arises primarily from site isolation as the polymer shields the reactive core moiety from deactivation. However, it is important that the dendritic polymer participates in some fashion in the catalysis in order to overcome the negative kinetic effects associated with encapsulation. One such mechanism involves substrate preconcentration. Substrate accumulation near the catalytic site is greatest with high generation dendrimers due to the more pronounced nanoenvironment obtained with these materials. This effect is usually the direct result of the molecular design of the dendrimer where a gradient of polarity can be used to drive the reactants to the core of a dendrimer while expelling products back to the surrounding solvent. The phenomenon of substrate preconcentration in the interior of the dendrimer has been referred to as a “concentrator effect” while the thermodynamic driving force expelling products has been described as a “catalytic pump.” While in the confines of the dendritic interior, substrate-catalyst pairs are subject to dielectric effects exerted by the polymer support producing nanoenvironment effects that, in general, are not trivial. Indeed, they often dominate the overall activity and selectivity for a particular transformation. Finally, it has been shown that substrate selectivity can be engineered through steric restriction to an active site located at the core of the dendrimer; this effect manifests itself more clearly with the larger globular dendrimers since they provide the best opportunity for complete encapsulation.

For peripherally modified dendrimers, the dendrimer effect arises from various interactions involving neighboring catalytic sites or reactive groups in close proximity at the surface of the macromolecule. This effective means of confinement also affects the molecular interactions between the dendrimer and various substrates or co-catalysts at the dendrimer-solvent interface. Such interactions, in turn, affect the activity



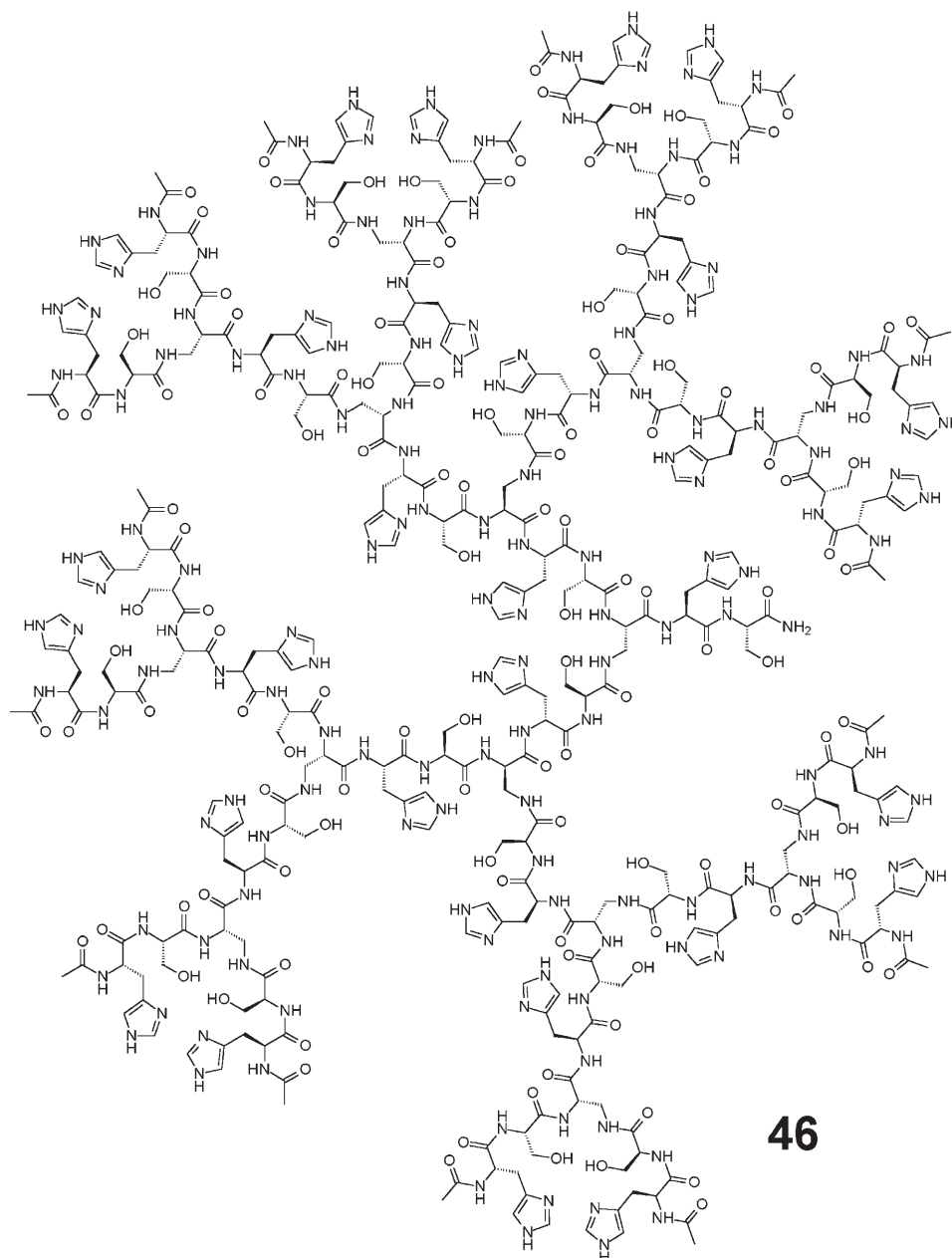


**Figure 12.** G4 peptide-dendrimer catalyst containing His-Ser consensus sequence for ester hydrolysis.

and selectivity profiles of the dendrimer catalysts. For example, cooperativity between proximal catalyst groups arises from steric confinement at the dendrimer periphery, although a strict relationship between larger dendrimer generations and optimal catalytic activity is not always established. Another consequence of catalyst immobilization on dendritic supports is the high local concentration of reactive groups within well-defined nanoscopic reaction volumes. This phenomenon can result in an autocatalytic activation of surface bound precatalysts that cannot be replicated in a randomly dispersed small molecule system. Finally, substrate selectivity can be achieved through spe-

cific interactions with the polymer: for example, chiral discrimination has been observed when enantiopure dendrimers are employed and ion pairing at the dendrimer surface can be used to discriminate between positively or negatively charged substrates.

## Acknowledgements

*This work was funded by the National Science Foundation (NSF-DMR0317514) and the Department of Energy through the Biomolecular Science Program at LBNL (DE-AC03-76SF00098).*

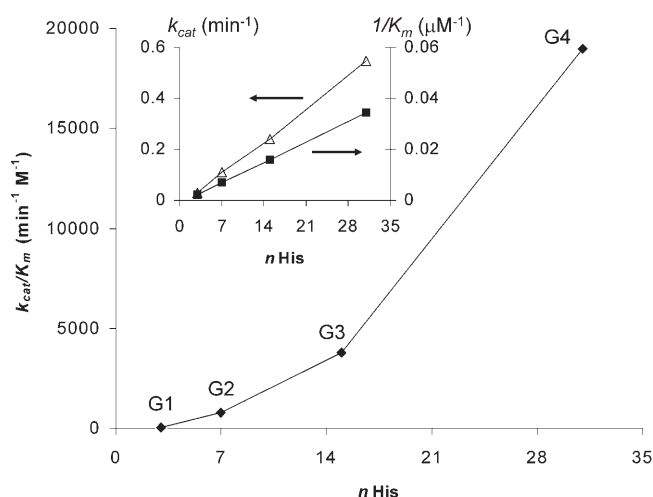


**Figure 13.** Reactivity of peptide dendrimers containing a His-Ser dipeptide at each generation expressed as a function of the number of His residues.

## References

- [1] M. Poliakoff, J. M. Fitzpatrick, T. R. Farren, P. T. Anastas, *Science* **2002**, 297, 807–810.
- [2] B. M. Trost, *Angew. Chem.* **1995**, 107, 285–317; *Angew. Chem. Int. Ed.* **1995**, 34, 259–281.
- [3] T. Frenzel, W. Solodenko, A. Kirschning, in: *Polymeric Materials in Organic Synthesis and Catalysis*, (Ed.: M. R. Buchmeiser), Wiley-VCH, Weinheim, **2003**, pp. 201–240.
- [4] T. J. Dickerson, N. N. Reed, K. D. Janda, *Chem. Rev.* **2002**, 102, 3325–3344.
- [5] R. Haag, S. Roller, in: *Polymeric Materials in Organic Synthesis and Catalysis*, (Ed.: M. R. Buchmeiser), Wiley-VCH, Weinheim, **2003**, pp. 305–344.
- [6] a) R. van Heerbeek, P. C. J. Kamer, P. W. M. N. van Leeuwen, J. N. H. Reek, *Chem. Rev.* **2002**, 102, 3717–3756; b) D. Astruc, F. Chardac, *Chem. Rev.* **2001**, 101, 2991–3024.
- [7] D. de Groot, B. F. M. de Waal, J. N. H. Reek, A. P. H. J. Schenning, P. C. J. Kamer, E. W. Meijer, P. W. N. M. van Leeuwen, *J. Am. Chem. Soc.* **2001**, 123, 8453–8458.
- [8] a) M. Ooe, M. Murata, A. Takahama, T. Mizugaki, K. Ebitani, K. Kaneda, *Chem. Lett.* **2003**, 32, 692–693; b) T. Mizugaki, Y. Miyauchi, M. Murata, K. Ebitani, K. Kaneda, *Chem. Lett.* **2005**, 34, 286–287.
- [9] a) N. Brinkmann, D. Giebel, G. Lohmer, M. T. Reetz, U. Kragl, *J. Catal.* **1999**, 183, 163–168; b) D. de Groot, J. C. de Wilde, R. J. van Haaren, J. N. H. Reek, P. C. J. Kamer, P. W. N. M. van Leeuwen, E. B. Eggeling, D. Vogt, H. Kooijman, A. L. Spek, A. W. van der Made, *Chem. Commun.* **1999**, 1623–1624; c) D. de Groot, J. N. H. Reek, P. C. J. Kamer, P. W. N. M. van Leeuwen, *Eur. J. Org. Chem.* **2002**, 6, 1085–1095.
- [10] a) *Dendrimers and Other Dendritic Polymers*, (Eds.: J. M. J. Fréchet, D. A. Tomalia), John Wiley & Sons, Chichester, **2001**; b) *Dendrimers and Dendrons*, (Eds.: G. R. Newkome, C. N. Moorefield, F. Vögtle), Wiley-VCH, Weinheim, **2004**.
- [11] a) R. B. Merrifield, *J. Am. Chem. Soc.* **1963**, 85, 2149–2154; b) R. B. Merrifield, *Science* **1965**, 150, 178–185.
- [12] a) C. J. Hawker, J. M. J. Fréchet, *J. Am. Chem. Soc.* **1990**, 112, 7638–7647; b) S. M. Grayson, J. M. J. Fréchet, *Chem. Rev.* **2001**, 101, 3819–3868.
- [13] a) D. A. Tomalia, H. Baker, J. Dewald, M. Hall, G. Kallos, S. Martin, J. Roeck, J. Ryder, P. Smith, *Polymer J.* **1985**, 17, 117–132; b) G. R. Newkome, Z. Yao, G. R. Baker, V. K. Gupta, *J. Org. Chem.* **1985**, 50, 2003–2004.
- [14] a) C. J. Hawker, R. Lee, J. M. J. Fréchet, *J. Am. Chem. Soc.* **1991**, 113, 4583–4588; b) A. Hult, M. Johansson, E. Malmström, *Adv. Polym. Sci.* **1999**, 143, 1–34; c) M. Bednarek, T. Biedron, J. Helinski, K. Kaluzynski, P. Kubisa, S. Penczek, *Macromol. Rapid Commun.* **1999**, 20, 369–372.
- [15] a) K. Matyjaszewski, P. J. Miller, J. Pyun, G. Kickelbick, S. Diamanti, *Macromolecules* **1999**, 32, 6526–6535; b) A. W. Bosman, R. Vestberg, A. Heumann, J. M. J. Fréchet, C. J. Hawker, *J. Am. Chem. Soc.* **2003**, 125, 715–728; c) M. Kamigaito, T. Ando, M. Sawamoto, *Chem. Rev.* **2004**, 4, 159–175; d) V. Darcos, A. Dureault, D. Taton, Y. Gnanou, P. Marchand, A.-M. Caminade, J.-P. Majoral, M. Destarac, F. Leising, *Chem. Commun.* **2004**, 2110–2111.
- [16] a) A. D. Schlüter, J. P. Rabe, *Angew. Chem. Int. Ed.* **2000**, 39, 864–883; b) S. M. Grayson, J. M. J. Fréchet, *Macromolecules* **2001**, 34, 6542–6544; c) T.-L. Choi, J. M. J. Fréchet, *Polym. Mater. Sci. Eng.* **2004**, 91, 199; d) B. Helms, J. L. Mynar, C. J. Hawker, J. M. J. Fréchet, *J. Am. Chem. Soc.* **2004**, 126, 15020–15021.
- [17] a) D. A. Tomalia, A. M. Naylor, W. A. Goddard, III, *Angew. Chem. Int. Ed.* **1990**, 29, 138–175; b) A. W. Bosman, H. M. Janssen, E. W. Meijer, *Chem. Rev.* **1999**, 99, 1665–1688; c) V. Percec, W.-D. Cho, G. Ungar, *J. Am. Chem. Soc.* **2000**, 122, 10273–10281; d) C. J. Hawker, P. J. Farrington, M. E. Mackay, K. L. Wooley, J. M. J. Fréchet, *J. Am. Chem. Soc.* **1995**, 117, 4409–4410.
- [18] a) C. J. Hawker, J. M. J. Fréchet, *Macromolecules* **1990**, 23, 4726–4729; b) K. L. Wooley, C. J. Hawker, J. M. J. Fréchet, *J. Chem. Soc., Perkin Trans. 1* **1991**, 1059–1076; c) A. W. Freeman, L. A. J. Christoffels, J. M. J. Fréchet, *J. Org. Chem.* **2000**, 65, 7612–7617; d) Z. Bo, A. Schafer, P. Franke, A. D. Schlüter, *Org. Lett.* **2000**, 2, 1645–1648; e) J. M. Serin, D. W. Brousmiche, J. M. J. Fréchet, *Chem. Commun.* **2002**, 2605–2607; f) W. R. Dichtel, S. Hecht, J. M. J. Fréchet, *Org. Lett.* **2005**, 7, 4451–4454.
- [19] D. A. Tomalia, J. R. Dewald, (Dow Chemical Co.), US Patent 4,507,466, **1985**.
- [20] E. M. M. de Brabander-van den Berg, E. W. Meijer, *Angew. Chem.* **1993**, 105, 1370–1373; *Angew. Chem. Int. Ed.* **1993**, 32, 1308–1311.
- [21] C. Hawker, J. M. J. Fréchet, *Chem. Commun.* **1990**, 1010–1013.
- [22] H. Ihre, O. L. Padilla De Jesus, J. M. J. Fréchet, *J. Am. Chem. Soc.* **2001**, 123, 5908–5917.
- [23] a) H. Uchida, Y. Kabe, K. Yoshino, A. Kawamata, T. Tsumuraya, S. Masamune, *J. Am. Chem. Soc.* **1990**, 112, 7077–7079; b) A. W. van der Made, P. W. N. M. van Leeuwen, *Chem. Commun.* **1992**, 1400–1401; c) L. L.

- Zhou, J. Roovers, *Macromolecules* **1993**, 26, 963–968; d) S. W. Kraska, D. Seyferth, *J. Am. Chem. Soc.* **1998**, 120, 3604–3612; e) R. van Heerbeek, P. C. J. Kamer, P. N. M. W. van Leeuwen, J. N. H. Reek, *Org. Biomol. Chem.* **2006**, 4, 211–223.
- [24] a) G. R. Newkome, R. K. Behera, C. N. Moorefield, G. R. Baker, *J. Org. Chem.* **1991**, 56, 7162–7167; b) G. R. Newkome, A. Nayak, R. K. Behera, C. N. Moorefield, G. R. Baker, *J. Org. Chem.* **1992**, 57, 358–362; c) G. R. Newkome, C. D. Weis, C. N. Moorefield, *Macromolecules* **1997**, 30, 2300–2304; d) M. Brettreich, A. Hirsch, *Synlett* **1998**, 1396–1398; e) G. R. Newkome, K. K. Kotta, C. N. Moorefield, *J. Org. Chem.* **2005**, 70, 4893–4896.
- [25] A. Zubia, F. P. Cossio, I. Morao, M. Rieumont, X. Lopez, *J. Am. Chem. Soc.* **2004**, 126, 5243–5252.
- [26] a) H.-F. Chow, C. C. Mak, *J. Org. Chem.* **1997**, 62, 5116–5127; b) G. E. Oosterom, R. J. van Haaren, J. N. H. Reek, P. C. J. Kamer, P. W. N. M. van Leeuwen, *Chem. Commun.* **1999**, 1119–1120; c) P. B. Rheiner, D. Seebach, *Chem. Eur. J.* **1999**, 5, 3221–3236; d) T. Habicher, F. Diederich, V. Gramlich, *Helv. Chim. Acta* **1999**, 82, 1066–1095; e) M. Malkoch, K. Hallman, S. Lutsenko, A. Hult, E. Malmström, C. Moberg, *J. Org. Chem.* **2002**, 67, 8197–8202; f) R. Andrés, E. de Jesús, F. J. de La Mata, J. C. Flores, R. Gómez, *Eur. J. Inorg. Chem.* **2002**, 2281–2286.
- [27] G. E. Oosterom, S. Steffens, J. N. H. Reek, P. C. J. Kamer, P. W. N. M. van Leeuwen, *Top. Catal.* **2002**, 19, 61–73.
- [28] S. Hecht, J. M. J. Fréchet, *Angew. Chem. Int. Ed.* **2001**, 40, 74–91.
- [29] A. W. Herrmann, *Angew. Chem. Int. Ed.* **2002**, 41, 1290–1309.
- [30] T. Fujihara, Y. Obora, M. Tokunaga, H. Sato, Y. Tsuji, *Chem. Commun.* **2005**, 4526–4528.
- [31] D. M. Singleton, (Shell Oil Corp.), US Patent 4,472,522, **1985**; *Chem. Abstr.* **1985**, 102, 46405.
- [32] C. Müller, L. J. Ackerman, J. N. H. Reek, P. C. J. Kamer, P. W. N. M. van Leeuwen, *J. Am. Chem. Soc.* **2004**, 126, 14960–14963.
- [33] a) C. J. Hawker, K. L. Wooley, J. M. J. Fréchet, *J. Am. Chem. Soc.* **1993**, 115, 4375–4376; b) J. F. G. A. Jansen, E. M. M. de Brabander van den Berg, E. W. Meijer, *Science* **1994**, 266, 1226–1229; c) J. F. G. A. Jansen, E. W. Meijer, E. M. M. de Brabander-van den Berg, *J. Am. Chem. Soc.* **1995**, 117, 4417–4418.
- [34] C. Liang, J. M. J. Fréchet, *Prog. Polym. Sci.* **2005**, 30, 385–402.
- [35] X. Zhang, H. Xu, Z. Dong, Y. Wang, J. Liu, J. Shen, *J. Am. Chem. Soc.* **2004**, 126, 10556–10557.
- [36] G. Muges, H. B. Singh, *Chem. Soc. Rev.* **2000**, 29, 347–357.
- [37] D.-L. Jiang, C.-K. Choi, K. Honda, W.-S. Li, T. Yuzawa, T. Aida, *J. Am. Chem. Soc.* **2004**, 126, 12084–12089.
- [38] a) A. R. Vaino, D. B. Goodin, K. D. Janda, *J. Comb. Chem.* **2000**, 2, 330–336; b) S. W. Gerritz, *Curr. Opin. Chem. Biol.* **2001**, 5, 264–268.
- [39] M. E. Piotti, F. Rivera, Jr., R. Bond, C. J. Hawker, J. M. J. Fréchet, *J. Am. Chem. Soc.* **1999**, 121, 9471–9472.
- [40] S. Hecht, J. M. J. Fréchet, *J. Am. Chem. Soc.* **2001**, 123, 6959–6960.
- [41] T. Mizugaki, C. E. Hetrick, M. Murata, K. Ebitani, M. D. Amiridis, K. Kaneda, *Chem. Lett.* **2005**, 34, 420–421.
- [42] M. Ooe, M. Murata, T. Mizugaki, K. Ebitani, K. Kaneda, *J. Am. Chem. Soc.* **2004**, 126, 1604–1605.
- [43] a) C. O. Liang, B. Helms, C. J. Hawker, J. M. J. Fréchet, *Chem. Commun.* **2003**, 20, 2524–2525; b) B. Helms, C. O. Liang, C. J. Hawker, J. M. J. Fréchet, *Macromolecules* **2005**, 38, 5411–5415.
- [44] a) G.-J. Deng, Q.-H. Fan, X.-M. Chen, G.-H. Liu, *J. Mol. Catal. A: Chem.* **2003**, 193, 21–25; b) G.-J. Deng, B. Yi, Y.-Y. Huang, W.-J. Tang, Y.-M. He, Q.-H. Fan, *Adv. Synth. Catal.* **2004**, 346, 1440–1444.
- [45] a) P. Bhyrappa, J. K. Young, J. S. Moore, K. S. Suslick, *J. Mol. Catal. A: Chem.* **1996**, 113, 109–116; b) P. Bhyrappa, J. K. Young, J. S. Moore, K. S. Suslick, *J. Am. Chem. Soc.* **1996**, 118, 5708–5711.
- [46] R. M. Crooks, M. Zhao, L. Sun, V. Chechik, L. K. Yeung, *Acc. Chem. Res.* **2001**, 34, 181–190.
- [47] S. V. Aathimaniandan, B. S. Sandanaraj, C. G. Arges, C. J. Bardeen, S. Thayumanavan, *Org. Lett.* **2005**, 7, 2809–2812.
- [48] J.-J. Lee, W. T. Ford, J. A. Moore, Y. Li, *Macromolecules* **1994**, 27, 4632–4634.
- [49] Y. Pan, W. T. Ford, *Macromolecules* **2000**, 33, 3731–3738.
- [50] L. Liu, R. Breslow, *J. Am. Chem. Soc.* **2002**, 124, 4978–4979.
- [51] L. Liu, M. Rozenman, R. Breslow, *J. Am. Chem. Soc.* **2002**, 124, 12660–12661.
- [52] L. Liu, R. Breslow, *Biorg. Med. Chem.* **2004**, 12, 3277–3287.
- [53] L. Liu, R. Breslow, *J. Am. Chem. Soc.* **2003**, 125, 12110–12111.
- [54] a) K.-D. Hungenberg, J. Kerth, F. Langhauser, H.-J. Müller, P. Müller, *Angew. Makromol. Chem.* **1995**, 227, 159–177; b) Brintzinger, H. H.; Fischer, D.; Mülhaupt, R.; Rieger, B.; Waymouth, R. M. *Angew. Chem.* **1995**, 107, 1255–1283; *Angew. Chem. Int. Ed.* **1995**, 34, 1143–1170.
- [55] M. Mager, S. Becke, H. Windisch, U. Denninger, *Angew. Chem. Int. Ed.* **2001**, 40, 1898–1902.
- [56] Z. J. Zheng, J. Chen, Y.-S. Li, *J. Organomet. Chem.* **2004**, 689, 3040–3045.
- [57] Z. Guan, P. M. Cotts, E. F. McCord, S. J. McLain, *Science* **1999**, 283, 2059–2062.
- [58] a) D. P. Gates, S. A. Svejda, E. Onate, C. M. Killian, L. K. Johnson, P. S. White, M. Brookhart, *Macromolecules* **2000**, 33, 2320–2334; b) M. D. Leatherman, S. A. Svejda, L. K. Johnson, M. Brookhart, *J. Am. Chem. Soc.* **2003**, 125, 3068–3081.
- [59] J. M. Benito, E. de Jesús, F. J. de La Mata, J. C. Flores, R. Gómez, *Chem. Commun.* **2005**, 5217–5219.
- [60] a) L. Ropartz, R. E. Morris, D. J. Cole-Hamilton, D. F. Foster, *Chem. Commun.* **2001**, 361–362; b) L. Ropartz, K. J. Haxton, D. F. Foster, R. E. Morris, A. M. Z. Slawin, D. J. Cole-Hamilton, *J. Chem. Soc., Dalton Trans.* **2002**, 4323–4334.
- [61] R. Breinbauer, E. N. Jacobsen, *Angew. Chem. Int. Ed.* **2000**, 39, 3604–3607.

- [62] a) C. Francavilla, F. V. Bright, M. R. Detty, *Org. Lett.* **1999**, *1*, 1043–1046; b) M. D. Drake, F. V. Bright, M. R. Detty, *J. Am. Chem. Soc.* **2003**, *125*, 12558–12566.
- [63] J. Kofoed, J.-L. Reymond, *Curr. Opin. Chem. Biol.* **2005**, *9*, 656–664.
- [64] C. Douat-Casassus, T. Darbre, J.-L. Reymond, *J. Am. Chem. Soc.* **2004**, *126*, 7817–7826.
- [65] E. Delort, T. Darbre, J.-L. Reymond, *J. Am. Chem. Soc.* **2004**, *126*, 15642–15643.
-